[redacted]

ORNL
MASTER COPY

ORNL
Central Files Number
51-10-70 Part I
Revised

INTRODUCTION TO SHIELD DESIGN

DECLASSIFIED
Per Letter Instructions
TID 1117
H. Stokes
For N. T. Bray, Supervisor
Laboratory Records Dept.
ORNL

OAK RIDGE NATIONAL LABORATORY
OPERATED BY
CARBIDE AND CARBON CHEMICALS COMPANY
A DIVISION OF UNION CARBIDE AND CARBON CORPORATION
UCC
POST OFFICE BOX P
OAK RIDGE, TENNESSEE

[redacted]

[redacted]

ORNL
Central Files Number
51-10-70
Part I - Revised
This document consists of 68
pages. Copy 173 of 216. Series A

OAK RIDGE NATIONAL LABORATORY

INTRODUCTION TO SHIELD DESIGN

E. P. Blizard

Part One

The Sources of Radiation

The Attenuation Processes

Geometry of Shielding

January 30, 1952

This article is to be the basis for a chapter in a Reactor Technology textbook being edited by Samuel Glasstone and Neal F. Lansing.

[redacted]

[redacted]

[redacted]

INTERNAL DISTRIBUTION

1. E. P. Blizard
2. R. C. Briant
3. C. E. Clifford
4. H. L. F. Endlund
5. A. P. Fraas
6-15. N. F. Lansing
16. F. K. McGowan
17. J. L. Meem
18. F. J. Muckenthaler
19. F. H. Murray
20. J. D. Flynn
21. T. V. Blosser
22. H. E. Hungerford
23. J. M. Miller
24. G. T. Chapman
25. F. N. Watson
26. R. G. Cochran
27. F. C. Maienschein
28. J. K. Leslie
29. G. M. McCammon
30. M. P. Haydon
31. M. K. Hullings
32. E. B. Johnson
33. K. M. Henry
34. R. H. Ritchie
35. A. Simon
36. A. H. Snell
37. A. M. Weinberg
38. E. O. Wollan
39. C. L. Storrs
40-89. Central Files
90-189. ORSORT Files
190. Physics Library

EXTERNAL DISTRIBUTION

191. H. A. Bethe - Cornell University
192. W. L. Carss - USAF, Oak Ridge
193. C. F. deGanahl - Pratt and Whitney Aircraft Corporation
194. J. R. Dietrich - Argonne National Laboratory
195. M. Fox - Brookhaven National Laboratory
196. K. Kasschau - AEC, Oak Ridge
197. C. R. Horner - AEC, Washington
198. E. O. Meals - AEC, Washington
199. T. Rockwell - Bureau of Ships
200-202. J. R. Hood - Wright Air Development Center
203. B. F. Ruffner - Boeing Airplane Company
204. J. H. Smith - Knolls Atomic Power Laboratory
205. H. E. Stone - Knolls Atomic Power Laboratory
206. H. E. Stern - Consolidated Vultee Aircraft
207. F. A. Cleveland - Lockheed Aircraft Corporation
208. J. J. Taylor - Westinghouse Electric Corporation
209. A. F. Thompson - AEC, Washington
210-211. G. Thornton - GE-ANP
212. L. Tonks - Knolls Atomic Power Laboratory
213. G. Young - NDA
214. R. Zirkind
215-216. Technical Information Service, Oak Ridge

[redacted]

[redacted]

[redacted]

TABLE OF CONTENTS

INTRODUCTION TO SHIELD DESIGN

Part I	Page No.
A. THE SOURCES OF RADIATION	8
1. Introductory Survey	8
2. Fission Neutrons	11
a. Prompt Neutrons	11
b. Delayed Neutrons	13
3. Prompt Fission Gammas	14
4. Delayed Gammas from Fission Fragments	14
5. Capture Gamma Rays	17
6. Inelastic Scattering Gammas	21
B. THE ATTENUATION PROCESSES	22
1. Neutron Cross Sections	23
a. Absorption	23
b. Elastic Scattering	24
c. Inelastic Scattering	25
d. Hydrogen Cross Section	27
e. The Effective Removal Cross Section	28
f. The Lightest Neutron Shield	29
2. Gamma-ray Cross Sections	29
a. Photoelectric Effect	29
b. Compton Effect	30
c. Pair Production	32

[redacted]

[redacted]

Page No.

3. The Relative Importance of the Gamma Interaction Processes 33

a. Hydrogen 33

b. Other Light Elements 33

c. Heavy Elements 33

4. Gamma Energy-Absorption Cross Section 37

C. GEOMETRY OF SHIELDING 40

1. The Simple Geometries 40

a. Plane Collimated Source 40

b. Inverse Square Law 42

c. Point Source and Spherical Shield 42

2. Type of Detector 43

a. Directional Detector 43

b. Isotropic Detector 43

3. General Transformations for Unspecified Attenuation Functions 44

a. Point to Point Attenuation Kernel 44

b. Plane Isotropic Source in Infinite Medium 45

c. Plane to Sphere Transformation 52

d. Plane to Cylinder Transformation 54

4. Geometry for Partially Specified Attenuation Functions 56

5. Geometry for the Simple Attenuation Functions 59

[redacted]

[redacted]

Page No.

6. Slab Geometry 59

a. Isotropic Plane Source 60

1) Exponential Attenuation, Directional Detector 61

2) Exponential Attenuation, Milligoat Detector 61

3) Linear Buildup, Directional Detector 61

b. Shielded Semi-infinite Volume-Distributed Source 62

c. Unshielded Semi-infinite Volume-Distributed Source 69

7. Line Source 66

a. Line Source, Milligoat, Exponential Attenuation with Linear Buildup Factor 66

D. REFERENCES 68

- - -

[redacted]

LIST OF TABLES

Table No.	Title	Page No.
1	Delayed Neutrons	13
2	Fission Gammas	14
3	Delayed Gammas from U^{235} Fission Products	15
4	Fission Fragment Hard Gamma Emitters	16
5	Capture Gamma-ray Data	20
6	Effective Removal Cross Sections	28
7	Minima in Total Gamma Cross Section	34

ABSTRACT

The sources of radiation which are of interest for shield design are described in some detail. Convenient forms of the fission neutron spectrum are given, but detailed gamma-ray information is confined to the references. The attenuation processes which are used in shielding are described individually, and their relative importance is discussed. Some of the simpler geometrical transformations which are useful in applying experimental information to shield design are derived and illustrated. In addition, some of the basic attenuation forms are applied to common configurations such as are used in reactor shielding.

- - -

INTRODUCTION TO SHIELD DESIGN

E. P. Blizard

THE SOURCES OF RADIATION

Introductory Survey

The shielding of nuclear reactors involves attenuations of seldom less than six and occasionally as many as twelve factors of ten. There are two general consequences of this fact. In the first place, this means that the particles or photons which penetrate the shield are very unusual, so that the sources must be examined in considerable detail for components which, although negligible within the reactor, might be dominant outside the shield. In the second place, mechanisms whereby the shield is circumvented, as by the removal of a control rod which has become radioactive, can be all-important if not anticipated. For these reasons the first part of this chapter will be devoted to a careful description of the several sources of radiation, all of which, of course, stem from the fission process itself.

The penetrating radiations are of course gamma rays and fast neutrons, and attention will be focused on these, but the other less penetrating components such as thermal neutrons which in some cases can give rise to penetrating radiations, e.g. capture gamma rays, must also be discussed.

Figure 1, Genealogy of Radiations for Shielding, shows the many sources of penetrating radiation which must be checked off before a shield design is complete. Accompanying the fission process itself is a burst of gamma rays, of total energy about 5 Mev. From the fission fragments come almost at once the hard "prompt fission neutrons," on the average 2 1/2 per fission. With varying radioactive decay periods come the "delayed neutrons" from certain of the fission fragments. These are softer and less plentiful by a factor of

UNCLASSIFIED
DWG. 10991A

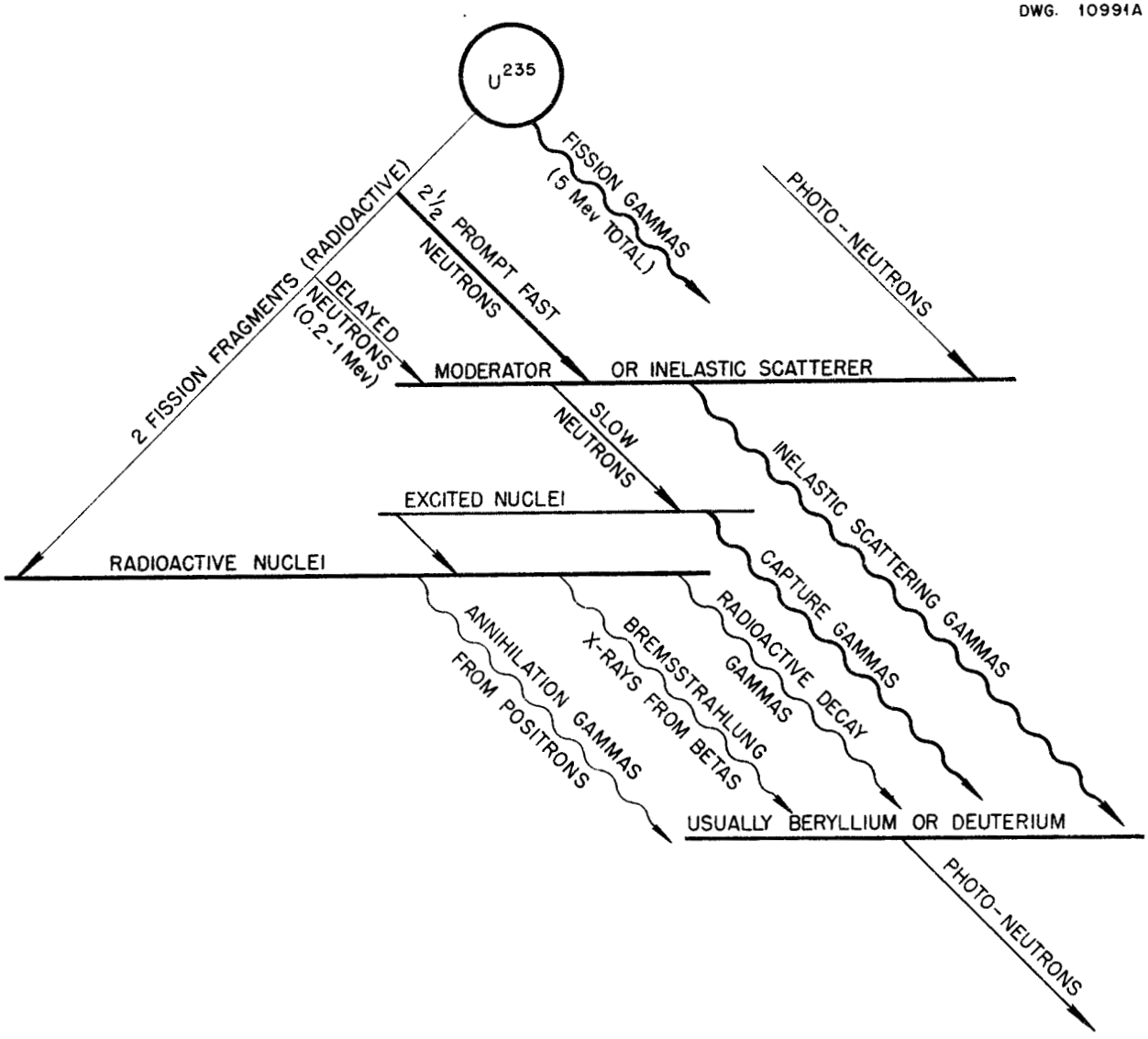

Fig. 1. Genealogy of Radiations for Shielding.

greater than one hundred. In addition, gamma rays will also be emitted from most of the fission fragments in radioactive decay. This will usually occur in a direct emission from the nucleus, but it must also be remembered that any positrons emitted will give rise to annihilation gamma radiation of at least one half Mev, and that energetic beta particles of either sign can produce bremsstrahlung on slowing down.

The fast fission neutrons in addition to contributing heavily as such to biological dose, can give rise to secondary gamma rays wherever they are stopped, either by inelastic scattering in the slowing down process, or by capture, usually at very low neutron energies. In either case the scattering or capturing nucleus emits considerable gamma radiation, which is in itself both penetrating and biologically important. Subsequent to the capture gamma rays, which are emitted at once, it is common for a further radioactive decay to take place.

The genealogy is not complete without mention of photoneutrons, which are usually negligible, but in certain cases can be very important. These neutrons result from the interaction of a rather high energy gamma ray with a nucleus. Since the threshold for the reaction is in general quite large, about 6 Mev, and since the cross section for the process is in most cases less than one thousandth of the total atomic cross section, the photoneutron production is not often high. There are two exceptions to the high threshold rule, these being deuterium at 2 1/4 Mev, and beryllium at 1.6 Mev. These materials deserve special attention in many shield designs.

We may expect to find, in general, all of these radiations produced within the reactor core itself. In this region the only important neutron source during reactor operation is the prompt fissions. After shutdown either delayed neutrons or photoneutrons or both can be important. Gamma

sources of most importance during operation are probably capture gammas, fission gammas and in certain cases inelastic scattering gammas. After shutdown, gammas will come from radioactive fission fragments, from induced radioactivity of components, and from capture gammas of delayed neutrons and photoneutrons.

The radiations which penetrate the shield around the reactor are predominantly the fast fission neutrons and their inelastic scattering and capture gamma rays which are produced in the shield. In some cases core gammas are also of importance or even dominant.

In addition to the direct penetration, there are other ways by which the radiations can reach sensitive areas. In general reactors must be cooled, and the coolants become radioactive on passage through the reactive region. This of course means that the whole circuit must be gamma-shielded. In some cases the fuel itself is also circulated so that fission fragments are found throughout the coolant circuit. Then delayed neutrons are also to be expected, and these may in turn activate a secondary coolant circuit.

Furthermore there are in general quite a few mechanical communications from the reactor core to the outside such as removable control rods, instruments, samples, etc. Adequate provision must be made for each of these.

The individual sources will now be discussed in more detail.

Fission Neutrons

The fission products emit neutrons which are classed as "prompt" if the time between fission and emission is not measurable, and "delayed" if this is measurable. In most cases the prompt neutrons are much more important, since they are in general more energetic and more numerous.

Prompt Neutrons. The spectrum of prompt fission neutrons has been measured for U^{235} as well as Pu^{239}, the published work on the former being much

more complete. Bonner, Ferrell, and Rinehart[1] measured the prompt spectrum from 0.075 to 0.6 Mev, Hill[2] measured all neutrons (prompt as well as delayed) from 0.4 to 6 Mev, and Watt[3] covered the much less populous range from 3 to 17 Mev. Watt combined all three sets of data and fitted them quite adequately with his own variation of a formula originally proposed by Feather.[4] Watt's formula is

$$N(E)dE = \sqrt{\frac{2}{\pi e}} \sinh \sqrt{2E} \; e^{-E} \, dE \tag{1}$$

$N(E)dE$ = number of neutrons of energy E to E + dE, per neutron emitted.

E = neutron energy, Mev.

Norris Nereson[5] has measured the fission spectrum of Pu^{239} using photographic plates for the energy range from 1/2 to 8 Mev. His data are fitted fairly well by Watt's formula, but there seems to be a somewhat greater abundance of the higher energy neutrons. The statistical accuracy is not, however, adequate to certify a genuine difference. Nereson only measured five tracks beyond 6.5 Mev.

Since in most shields the attenuation is sufficient so that only the hardest neutrons penetrate the full thickness it is often permissible to use a simpler form of (1) which fits adequately in the high energies. Two of these are:

$$N(E)dE \doteq \frac{1}{\sqrt{2\pi e}} \; e^{-(E - \sqrt{2E})} dE \tag{2}$$

$$N(E)dE = 1.8 \; e^{-0.75E} \, dE \tag{3}$$

The last of these is not derived from (1) but is nevertheless not a bad approximation to the data from 4 to 12 Mev. It is adjusted to agree in magnitude and slope with (2) at 8 Mev. For a formula fitted to agree similarly

at any other energy E_o, the following is convenient:

$$N(E)dE = \frac{1}{\sqrt{2\pi e}} e^{\sqrt{\frac{E_o}{2}} - \left(1 - \frac{1}{\sqrt{2E_o}}\right)E} dE \quad . \tag{4}$$

This should not be used for E or E_o less than about 3 Mev.

Delayed Neutrons. Delayed neutrons are less energetic and less numerous, hence are important only in special cases, as for example in a homogeneous circulating fuel reactor. Here the fuel is quite radioactive in any case, so that it would not be introduced to an occupied region, but the delayed neutrons introduce the further difficulty that a coolant such as sodium will become radioactive in a fuel-to-coolant heat exchanger.

Hughes[6] has summarized information on the delayed neutrons in a manuscript for the Plutonium Project Report, and his table of yields is here reproduced:

Table 1 - Delayed Neutrons

Half life, sec	Energy, kev	Absolute yields per 10^4 neutrons emitted(prompt and delayed)		
		U^{235}	U^{233}	Pu^{239}
55.6	250	2.5	1.8	1.4
22.0	570	16.6	5.8	10.5
4.51	412	21.3	8.6	12.6
1.52	670	24.1	6.2	--
0.43	400	8.5	1.8	11.9
		73.0	24.2	36.4 Total

The term yield as used here refers to the total fraction of all neutrons emitted which are associated with a given period.

The fact that the neutrons appear with definite half lives which are discernible in the fission fragments from several parent nuclei seems to indicate that the periods must be associated with certain radioactive nuclei. Indeed the 55.6 second period seems to be associated with the chemistry of Br^{87} and the 22 second period with that of I^{137}[7].

Prompt Fission Gammas

Just as in the case of neutrons, fission product gammas are also classed as "prompt" or "delayed," depending on whether the decay period is measurable or not. The term "fission gammas" is usually applied to the prompt emission, whereas the delayed radiation is always associated with the particular fission product emitter.

There have been two measurements of the gammas emitted in coincidence with the fission of U^{235}. The data are as follows:

Table 2 - Fission Gammas

	Total energy per fission	Average energy per photon
Deutsch and Rotblat[8]	5.1 ± 0.3 Mev	1 Mev
Kinsey, Hanna and Van Patter[9]	4.6 ± 0.1 Mev	2.5 Mev

The agreement on energy per fission is adequate, whereas that on the average energy per photon is not.

Delayed Gammas From Fission Fragments

Delayed gamma rays from the fission fragments are of considerable importance in the handling of reactors subsequent to shutdown. They have been examined by a number of authors, probably the most complete survey being that of Way and Wigner [10]. These investigators endeavored to find a rationale to describe in a general way the activities of the beta and gamma

emitters. Since there are so many possible modes of fission, it is to be expected that there must be some general conclusion to be drawn.

Although Way and Wigner were able to obtain an approximate relation between decay constant and beta energy per disintegration, there appeared no simple form for gamma energy per photon. Nevertheless it is in general true that the emitters of hard gammas are the less long-lived. This fact, however, is not very useful, since the average fission product suffers about three disintegrations before becoming stable, and a daughter of a long-lived parent is often short-lived and the emitter of a hard gamma.

The experimental data have been compiled by Way and Wigner and we reproduce a part of their table for gammas:

Table 3 - Delayed Gammas from U^{235} Fission Products

Rate, Mev/sec per fission	When valid	Reference
$0.90\ t^{-1.20}$	10 sec. 1 day	S. Katcoff, B. Finkle, N. Elliot, J. Knight, N. Sugarman, CC1128, Dec. 11, 1943
$4.2\ t^{-1.28}$	20 m - 3 days	L. Borst, CL-697. VIII,C4.
$49.0\ t^{-1.41}$	50 - 100 days	"
(t is in seconds)		

More recently, W. K. Ergen[11] has demonstrated that the longer lived hard gamma emitters are relatively few in number and fairly well known. By means of simple but careful computation he has succeeded in attributing the results of several experimental measurements of photoneutrons produced in Be or D to the hard gamma emitters of relatively few well known fission fragments. For many shielding problems the hard gammas are by far the more interesting, and for this reason a part of Ergen's table is here reproduced.

Table 4 - The Longer-lived Fission Fragment Hard Gamma Emitters

Nuclides[a)]	Half life[a)]	U^{235} fission yield %	Yield per decay, %	Energy
Ru^{106}, Rh^{106}	1 yr, 30 sec	0.48	2	2.9[b)]
Ce^{144}, Pr^{144}	275 days, 17.5 min	5.3	weak	>D[b)]
			2	2.185[b)]
			2	2.6[c)]
Eu^{156}	15.4 days	0.013	60	2[e)]
Ba^{140}, La^{140}	12.8 days, 40 hr	6.1	3.2	2.5[e)]
Te^{132}, I^{132}	77.7 hr[f)], 2.4 hr	4.5[f)]	2.7	2.0[g),h)]
Te^{131*}, Te^{131}	30 hr, 25 min	0.45[f)]	21.6	>D[h)]
I^{135}	6.7 hr	5.6	1.95	2.4[j)]
			4	1.8[i)]
Kr^{88}, Rb^{88}	2.77 hr, 17.8 min	3.1[k)]	<15	2.8[l)]
			19-34	1.85[l)]

a) If two entries occur they refer to parent and daughter, and the latter is the hard gamma emitter.

b) D. E. Alburger, E. der Mateosian, M. Goldhaber, S. Katcoff, Phys. Rev. 82, 332, (1951).

c) C. E. Mandeville, E. Shapiro, Phys. Rev. 79, 243, (1950).

d) L. Winsberg, paper 198 in Radiochemical Studies: The Fission Products, McGraw-Hill, N.Y., 1951.

e) B. Russell, D. Sachs, A. Wattenberg, R. Fields, Phys Rev. 73, 545, (1948).

f) A. C. Pappas and C. D. Coryell, Phys. Rev. 82, 329, (1951).

g) F. C. Maienschein, J. K. Bair, and W. B. Baker, private communication; G. W. Parker, private communication.

Table 4 - The Longer-lived Fission Fragment Hard Gamma Emitters (Cont.)

h) G. W. Parker, private communication.

i) H. A. Levy, M. H. Feldman, ORNL-286, p. 80.

j) A. D. Bogard and A. R. Brosi, ORNL-65, p. 59.

k) Interpolated value.

l) M. E. Bunker, L. M. Langer, R. J. D. Moffat, Phys. Rev. 81, 30, (1951).

In the use of Table 4 for shielding calculations it will always be necessary to multiply columns 3 and 4 to obtain gamma photons per 10^4 fissions. In the fifth column the symbol D implies that the gamma energy is greater than the deuterium photoneutron threshold, but otherwise not measured. The data are not suitable for use with times less than several hours after fission.

Capture Gamma Rays

When a neutron is captured by a nucleus, a new nucleus is formed in an excited state. The excitation energy, called the binding energy of the new nucleus, is dissipated almost at once ($\sim 10^{-13}$ seconds) by the emission in most cases of one or more gamma ray photons. Since the binding energies are large in general (~ 8 Mev) this effect is of considerable importance in shielding. It is especially important since these radiations are produced throughout the shield and even outside it, so that they do not, as is the case with gammas originating in the core, traverse the shield before reaching sensitive areas.

It is important in shield design so to choose and distribute materials that the capture gamma contribution to the biological dose outside is not more than, say, half of the total. Conversely, it is unnecessary to

suppress them to less than a few per cent. In order effectively to accomplish this, it is necessary to know at least approximately the spectra of capture gammas.

There have been a number of measurements of spectra, notably by Kinsey, Bartholomew, and Walker, at Chalk River, by Hamermesh at Argonne National Laboratory, and by Millar, Cameron, and Glicksman of Chalk River. (See Table 5 for capture gamma ray bibliography.)

Kinsey's group uses a pair spectrometer, which enables them to obtain detailed information about the energies involved. The determination of relative intensities has been more difficult but seems now to be well in hand. Kinsey's latest efforts have been directed in part toward determining the absolute number of photons per unit energy interval per neutron captured, and of course this is the essential number for shielding. Relative intensities which were at first reported by all investigators left some doubt, since low energy gammas and those internally converted were not measured.

Both Hamermesh and Millar, Cameron and Glicksman used deuterium-loaded photographic plates, in which the photo-proton tracks were measured. This technique, being cruder than Kinsey's, does not reveal the spectral lines so clearly. Nevertheless, the sensitivity of the method is more easily calculated, and the detail is adequate for most shielding work.

Both of the foregoing techniques become unsatisfactory for measuring energies less than 3 to 4 Mev, and this is unfortunate since the minimum in the lead gamma cross section occurs at about 3 1/2 Mev. There seems to be room for investigations using the scintillation counter techniques which operate well to much lower energies. A start with this instrument is evident in the recent work of Pringle and Isford at the University of Manitoba, although they have not exploited the low-energy sensitivity of the method.

In addition to the spectral measurements mentioned above, there has been some interesting work by C. O. Muehlhause, of Argonne National Laboratory, to determine approximately the average number of photons which are emitted per neutron capture. Since the total energy available (the binding energy) is fairly well known, Muehlhause's data gives a fair indication of the general spectral shape.

From the shielding point of view, capture gamma-ray spectra fall into three classes

1) the ground-state transition giving the most energetic photon is dominant,
2) the gammas are smeared out, usually peaking at about half the maximum energy,
3) they are weak or nonexistent because of strongly competing particle emission.

In Table 5 are listed the spectra which have been studied, together with an indication of the type of spectrum according to the categories of the foregoing paragraph, and the binding energy where measured. The isotopes indicated are the target nuclei before neutron capture. The data on spectral type and binding energy are in each case taken from the first listed reference.

It is to be noted from the table that most elements give multiple capture gammas. These photons, moreover, are often most numerous at the energy where the heavy element gamma cross sections are minimum. Probably the most interesting data are for boron and lithium*, which fall into class 3) and hence are very desirable shield components. It is fortunate that these

* Nitrogen could also be included since in about 95% of the captures it gives a proton and no gammas, but its cross section for capture is relatively low (1.7 b.), so that its virtue in this respect is relatively unimportant.

TABLE 5 Capture-gamma-ray Data

Target Nucleus	Spectral Type[a]	Binding Energy,[b] mev	References
H^1	1	2.23	(c)
Li^6	3	-	(d)
Be^9	1	6.797 ± 0.008	(e)
B^{10}	3	-	(d)
C^{12}	1	4.948 ± 0.008	(e)
N^{14}	2	10.823 ± 0.012	(e)
F^{19}	1	6.60 ± 0.03	(f)
Na^{23}	2	6.961 ± 0.012	(f,g)
$Mg^{24,25,26}$	2	7.334 ± 0.012 (24)	(f)
Al^{27}	1	7.724 ± 0.10	(h,i,f)
$Si^{28,29,30}$	2	8.476 ± 0.13 (28)	(f)
P^{31}	2	7.94 ± 0.03	(o)
S^{32}	2	8.64 ± 0.02	(o)
Cl^{35}	2	8.56 ± 0.03	(o)
K^{39}	2	7.77 ± 0.03	(k,g,n)
Ca^{40}	2	-	(n)
Mn^{55}	1	7.25 ± 0.03	(j,i,k,l)
Fe^{56}	1	7.63 ± 0.01	(j,i,k)
Co^{59}	2	7.73 ± 0.04	(j,k)
Ni^{58}	1	9.01 ± 0.03	(k)
Ni^{60}	1	8.55 ± 0.03	(k)
$Cu^{63,65}$	1	7.91 ± 0.01 (63)	(k)
$Br^{79,81}$	2	8.5 – 9.0	(h)
$Ag^{107,109}$	2	~8.0	(j)
Cd^{113}	2	~7.5	(h,g)
In^{115}	2	7.0 – 7.5	(j)
La^{139}	2	7.5 – 8.0	(h)
W	2	7.4	(m)
Au^{197}	2	9.0 – 9.5	(h)
Hg	2	8.0 – 8.5	(h)
Pb^{206}	1	6.734 ± 0.008	(n)
Pb^{207}	1	7.380 ± 0.008	(n)
Bi^{209}	1	4.170 ± 0.015	(n)
U^{235}	2	~5	(p)

(a) 1, ground-state transition predominates; 2, ground-state transition does not predominate; 3, charged-particle reaction.

(b) Isotope assignment, if any, is indicated in parentheses.

(c) R. E. Bell and L. G. Elliott, "Gamma-Rays from the Reaction $H^1(n,\gamma)D^2$ and the Binding Energy of the Deuteron," *Phys. Rev.* 79, 282-285 (1950).

(d) W. F. Hornyak, T. Lauritsen, P. Morrison, and W. A. Fowler, "Energy Levels of Light Nuclei. III," *Revs. Modern Phys.* 22, 291, esp. 321 (1950).

(e) B. B. Kinsey, G. A. Bartholomew, and W. H. Walker, "γ-Rays Slow Neutron Capture in Beryllium, Carbon, and Nitrogen," *Can. J. Phys.* 29, 1-13 (1951).

(f) B. B. Kinsey, G. A. Bartholomew, and W. H. Walker, "Neutron Capture γ-Rays from Fluorine, Sodium, Magnesium, Aluminum, and Silicon," *Phys. Rev.* 83, 519-534 (1951).

(g) C. H. Millar, A. G. W. Cameron, and M. Glicksman, "Gamma-ray Studies Using Deuterium-loaded Photographic Plates," *Can. J. Res.* 28A, 475-487 (1950).

(h) B. Hamermesh, "Neutron Capture Gamma-Ray Spectra," *Phys. Rev.* 80, 415-419 (1950).

(i) B. Hamermesh, and V. Hummel, "Scintillation Counter Studies of Neutron Capture Gamma-Ray Spectra," *Phys. Rev.* 83, 663-664 (1951).

(j) B. Hamermesh, "Odd-Even Effect in Neutron Capture Gamma-Ray Spectra," *Phys. Rev.* 81, 487 (1951).

(k) B. B. Kinsey, G. A. Bartholomew, and W. H. Walker, "Transitions to the Ground States in Nuclei Excited by Slow Neutron Capture," *Phys. Rev.* 78, 481-482 (1950).

(l) R. W. Pringle and G. Isford, "Scintillation Spectroscopy of the Gamma-Rays from Slow Neutron Capture in Manganese," *Phys. Rev.* 83, 467-468 (1951).

(m) B. B. Kinsey, letter of Feb. 22, 1950 to E. P. Blizard.

(n) B. B. Kinsey, G. A. Bartholomew, and W. H. Walker, "Neutron Capture γ-Rays from Lead and Bismuth," *Phys. Rev.* 82, 380-388 (1951).

(o) B. B. Kinsey, G. A. Bartholomew, and W. H. Walker, "Neutron Capture γ-Rays from Phosphorus, Sulfur, Chlorine, Potassium, and Calcium," *Phys. Rev.* 85, 1012-1023 (1952).

(p) E. P. Blizard, estimate only, based on calculation of gamma intensity near to an MTR-type reactor. This is gamma-ray emission on thermal neutron non-fission capture, which constitutes 15.5% of all capture processes.

elements also have large absorption cross sections, so that a small addition of boron or lithium effects a considerable suppression of the capture gamma rays.

As might be expected from energy level density considerations, the type 1) spectra are confined for the most part to light elements and those few heavy elements which behave like light elements in this respect (magic nuclei).

Inelastic Scattering Gammas

When a neutron is captured to form a compound nucleus it is always possible that the excited nucleus so formed will pass to the ground state with the emission of a neutron. If the neutron entered with adequate kinetic energy, it is possible on the subsequent emission of a neutron that the residual nucleus be left in an excited state, which subsequently decays by the emission of one or more photons. This process, known as inelastic scattering, becomes increasingly probable the higher the kinetic energy of the neutron, since the density of allowed intermediate states (nuclear levels) is greater the higher the energy of the state.

Although the process has been observed for many years, not until recently have careful measurements been made of the gamma spectra, and as yet the data are very sparse[12-13]. Fortunately the photon emission is probably similar to that in the capture process, although the available energies are often lower, and this enables some prediction of spectra to be expected. Thus light elements and magic nuclei probably give harder inelastic scattering gammas than non-magic heavy nuclei, and then cross sections of inelastic scattering are probably correspondingly smaller.

THE ATTENUATION PROCESSES

Neutron Cross Sections

Nothing is more fundamental to the shielding problem than the cross sections themselves. We shall speak of microscopic and macroscopic cross sections. So that we may illustrate these two terms, consider a collimated beam of particles incident on a slab of material of infinitesimal thickness dx. The fraction which interact by process "α" (such as absorption, scattering, etc.) is then given by Σ_α dx, where Σ_α is the macroscopic cross section of the slab material for the given process. If several processes α, β, γ, etc. are possible, the total macroscopic cross section is the sum of all of these, i.e.

$$\Sigma_t = \Sigma_\alpha + \Sigma_\beta + \Sigma_\gamma + \ldots\ldots \tag{5}$$

A closer look at the slab material reveals that it is made up of atoms, and if there are N of these per unit volume, then the microscopic cross section is given by

$$\sigma_\alpha = \frac{\Sigma_\alpha}{N} \quad .$$

Note that the dimension of the macroscopic cross section is inverse length, whereas that of the microscopic cross section is length squared. The σ's are likewise additive, as are the N's if there are seveal types of atoms intermixed in the material. The cross section definition can be symbolized as follows

$$-\frac{dI}{I} = \Sigma_t \, dx \tag{6}$$

where I is the beam intensity in particles per unit area per unit time. The solution for equation (6) is the well known exponential

$$I(x) = I_o \, e^{-\Sigma_t x} \tag{7}$$

which expresses the current density of uncollided particles I(x) as a function of penetration distance x. For thick shields (x large) the expression for total penetration becomes much more complicated because of the necessity for taking into account the multiply scattered particles.

The several possible neutron-nucleus interactions are now investigated in more detail, paying special attention to their importance in shielding.

Absorption. In this process a neutron enters the nucleus and no neutron leaves. This would of course be the ideal way to shield out neutrons. Unfortunately the cross sections for this process are very low except for very slow neutrons, for which the non-absorber is the exception rather than the rule. Since the neutrons must be absorbed somehow in any shield, the process is resolved into first slowing down the fast neutrons, followed almost automatically by capture at low energy. It has never been necessary to add a material to ensure slow neutron capture.

It has already been mentioned that most nuclei on absorbing a neutron emit about 6 Mev of gamma rays. Since these must in turn be shielded out it is desirable to minimize this effect by proper choice of shield materials. For this purpose isotopes are chosen which emit charged particles instead of gamma photons, the class 3) isotopes of Table 5. The most important of these are B^{10} and Li^6, both of which are endowed with very high capture cross sections. The boron isotope gives one gamma photon in about 95% of the captures, but its energy is only 1/2 Mev, so it is easily stopped. Li^6 gives no observed gamma ray. Another isotope of this type is N^{14}, which gives only a proton on capturing a neutron. Unfortuantely, the absorption cross section for this isotope is low, and furthermore in one out of every 17 captures it gives 10.8 Mev of gammas.

Elastic Scattering. In this process the neutron "collides" with the nucleus and departs, leaving the total kinetic energy of neutron and nucleus unchanged. For all but thermal neutrons this involves a transfer of energy to the nucleus, the amount varying inversely with the mass. At low and intermediate energies the neutrons appear actually to join with the nucleus, leaving a short time later with the same velocity relative to the nucleus. The nucleus which is formed by the temporary addition of a neutron is called the "compound nucleus," and the important feature of the processes characterized by its formation is that the neutron suffers appreciable angular deviation. This has two important consequences. The simplest is that the scattering considerably lengthens the paths of neutrons through matter by making them tortuous. This of course is advantageous because it increases the probability of removal by further collisions and eventual absorption. The other consequence, which is of considerable importance in reactors as well, is the slowing-down of the neutron through energy transfer to the recoiling nucleus. Since in general all cross sections increase with decreasing energy, this moderation is a very important step toward neutron absorption. In a water shield, for example, a collision with hydrogen is tantamount to removal from the penetrating beam.

At high energies, that is about 5 Mev for heavy nuclei and 10 for light, another type of elastic scattering, the so-called shadow scattering, becomes dominant.* In this process the neutron wave properties become evident, resulting in diffraction around the target nucleus. The effect is exactly analogous to that observed with a parallel beam of visible light diffracted around a small coin. Due to constructive interference a bright spot can sometimes be observed in the center of the shadow.

We ignore potential elastic scattering, since at high energies it is unimportant compared to "shadow scattering," and at lower energies it can for purposes of shielding discussions be lumped with compound nucleus elastic scattering.

Diffraction of neutrons around nuclei becomes important only when the wave length is of the same order or smaller than the nuclear radius, that is when

$$\lambda\!\!\!^{-} = \frac{\hbar}{p} \gtrsim R \tag{8}$$

$\lambda = 2\pi\lambda\!\!\!^{-}$ = neutron wavelength

$h = 2\pi\hbar$ = Planck's constant

p = neutron momentum

At large neutron energies, that is, small wavelengths, the cross section for this process approaches the area of a disc of nuclear radius, that is

$$\sigma_e \rightarrow \pi R^2 \tag{9}$$

where

$$R \approx 1.41 \times 10^{-13} \sqrt[3]{A} \text{ cm} \quad . \tag{10}$$

Since the angle of scattering is seldom very great, ($\leq \lambda\!\!\!^{-}/R$), the degradation in energy is very small. As a consequence this process is not of much help in shielding.

It should be noted that in none of the elastic process is any secondary radiation analogous to capture gamma rays given off. This of course must be true from energy considerations alone.

<u>Inelastic Scattering.</u> This process differs from elastic scattering in that some of the kinetic energy of the colliding particles is converted into intrinsic energy of the scattering nucleus. The nuclear inelastic scattering process always involves the formation of a compound nucleus. This nucleus has an energy above its ground state which is a consequence not only of the usual neutron binding energy, but in addition includes most of the kinetic energy of the incident neutron. It does not include all of the neutron kinetic energy, since some appears as kinetic energy of the recoiling

nucleus. If the compound nucleus is at sufficiently high energy, it becomes possible for it to expel a low energy neutron followed by one or more gamma quanta as well. The latter are referred to as inelastic scattering gamma rays, and the whole interaction as inelastic scattering.

Whether or not the neutron will be ejected at a lower energy depends entirely on the availability of suitable nuclear energy levels, or allowed excited states, into which the resultant nucleus can fall. There are two general rules regarding the density of these allowed states. The larger the nucleus, that is the more particles it possesses, the greater is the number of allowed states below any given energy of excitation. Consequently it is a general rule that, for a given neutron energy, inelastic scattering is more probable on collsision with heavy nuclei than light. (In light hydrogen the process is non-existent). Thus the threshold for inelastic scattering in oxygen is about 6 Mev, whereas in uranium it is probably as low as a few hundred kilovolts. Exceptions to this rule are the so-called "magic nuclei," which behave more like light nuclei. Examples of this type are bismuth and lead.

The second general rule regarding energy levels is that they increase in both density and breadth with excitation energy. That is, the number of levels per unit energy interval increases with increasing excitation energy, as does the breadth of each level. As a consequence the inelastic scattering process increases in relative probability (over, for example, compound nucleus elastic scattering or absorption) with increasing neutron energy. As a consequence, for all nuclei except light hydrogen, the inelastic scattering cross section approaches the cross section for formation of the compound nucleus, which is at high energies just the " hard sphere" cross section.

$$\sigma_{in.} \rightarrow \pi R^2 \qquad (11)$$

E large

Inelastic scattering is of considerable importance in shielding. By this process even the very high energy neutrons are brought in a single collision to energies of the order of one Mev or less, from which hydrogen very easily reduces their energy to thermal, where they are absorbed.

Hydrogen Cross Section. Because hydrogen is unique in its importance to neutron shielding it is considered separately here. It has been mentioned that inelastic scattering is unknown in hydrogen. Nevertheless neutrons on colliding elastically with a proton (hydrogen nucleus) at rest can lose, with equal probabilities, all fractions of initial energy from none to all. On the average, half of the energy is lost. This is of course a very important event since the cross section increases with decreasing energy so that subsequent collisions become more and more closely spaced. The first collision is at the same time the most important and the most difficult to achieve.

A convenient formula for the hydrogen cross section has been derived by T. A. Welton[16] from basic nuclear data, and agreement with experimental data is remarkably good. A simplified version of this formula, also good up to 12 Mev, is the following

$$\sigma_H = \frac{10.97}{E + 1.66} \text{ barns.} \qquad (12)$$

This expression gives the total cross section, but shadow scattering from such a small nucleus is relatively unimportant in the interesting range of energies.

The Effective Removal Cross Section. Since in a hydrogenous shield a single energy-reducing collision -- either elastic scattering by hydrogen or inelastic scattering by any other nucleus -- effectively removes a neutron, it appears that attenuation calculations should be reducible to a simple exponential form. This is indeed true, but some allowance should be made for the deflections from shadow scattering. The importance of deflections will of course vary with such factors as the total shield attenuation (for very thin shields deflection is ineffective), the location in the shield at which the deflection occurs, etc. Fortunately a series of experiments on the Lid Tank at Oak Ridge National Laboratory gives reasonably good empirical information on the overall shielding effectiveness of several materials, notably iron, boron, and lead, as they are inserted in a water shield. From these data come the very useful "effective removal cross sections," which are by definition the cross sections which give the correct attenuation in a simple exponential calculation. Interpolation on the basis of known macroscopic cross sections gives a rather broad and useful collection of data, the best confirmed of which appear in Table 6. About one-third of the shadow scattering is effective, but this fraction decreases with increasing atomic number. This is to be expected, since most scatterings occur within an angle of about λ/R.

Table - 6 Effective Removal Cross Sections

Substance	Barns/atom
Oxygen	0.8
Iron	2.0
Lead	3.4
B_4C	0.9
Be	1.22

The Lightest Neutron Shield. No discussion of neutron cross sections would be complete without a discussion of which element makes the lightest neutron shield. Consider an element of atomic mass A. From equations (9) and (10) we deduce that the fast neutron cross section will be about proportional to $A^{2/3}$. On the other hand the number of atoms per pound of material will be inversely proportional to A. Thus the cross section per pound is proportional to $A^{2/3}/A$ or $A^{-1/3}$. Thus the greatest return, in attenuation for a given weight of material is to be had from the material of lowest atomic weight, that is, hydrogen. Roughly, hydrogen would be better than uranium by a factor of about $238^{1/3}$, or about 6, if (9) and (10) were applicable to hydrogen, which they are not. The variance is such as to favor hydrogen considerably more, so that it is about 40 times better than uranium. The expressions (9) and (10) are appropriate for oxygen, however, indicating that this is better than uranium by a factor $(238/16)^{1/3}$, or about 2.5.

Gamma-ray Cross Sections[17-20]

The three main processes by which gamma rays are attenuated in matter have been described elsewhere. Their relative importance for different gamma-ray photon energies and different materials will be discussed here. It should be noted that while neutron cross sections were determined generally by A, the atomic weight, gamma cross sections are expressed as functions of Z, the nuclear charge.

Photoelectric Effect. In this process the gamma ray photon transfers all its energy to one of the electrons in the material of the shield. This electron is threby ejected from the atom, and is slowed down by many coulomb interactions. When the atom readjusts an x-ray is emitted, but this is a relatively unimportant effect since the x-rays are of low energy and easily

absorbed, and furthermore most of them never even escape the atom.* For this reason the photoelectric effect can be treated as a genuine absorption process in shielding calculations, attenuation according to a simple exponential function.

The photoelectric cross section varies sharply from element to element, being proportional to Z^n, where n varies from about 4 for low gamma energies to about 5 for high gamma energies. The cross section also varies sharply with photon energy, decreasing sharply with increasing energy. The process is most important for low-energy gamma photons, generally less than 1 Mev.

Compton Effect. In this process the gamma photon interacts with an electron which is so loosely bound in an atom that it behaves as if it were free. The incident photon energy is then divided in a more or less arbitrary way between the electron and the scattered photon. This process is definitely not an absorption process, since the scattered photons are not necessarily very much degraded in energy, nor are they appreciably deflected. This defection in the process makes the simple exponential attenuation calculation a serious underestimate. The correction to the latter takes the form of a "buildup factor," by which the uncollided flux must be multiplied in order to obtain the total transmitted flux.

$$I(x,E) = I(0,E)\ B(x,E)\ e^{-\mu(E)x} \tag{13}$$

where $I(x,E)$ is the flux of photons of energy E at x,

$I(0,E)$ is assumed collimated flux on a uniform slab shield,

$B(x,E)$ is the buildup factor, unity for thin shields, but approximately μx for large thicknesses,

* They transfer their energy directly to another outer electron, which escapes and soon dissipates its energy in many small collisions. This ejected electron is referred to as an "Auger Electron," after its discoverer.

$\mu(E)$ is the macroscopic total cross section for gamma photons of energy E,

x is the thickness of shield.

The value of the buildup factor varies with many things, such as the photon energy, the shielding material, the total attenuation, and the nature of the detector. For energies of a few Mev, large attenuations, and a detector which records total energy flux, the buildup factor is more or less independent of material and about equal to the number of mean free paths traversed.

$$B(x,E) \approx \mu x. \tag{13a}$$

Since the Compton effect deals with the electrons alone, and does not depend on the nuclei, the cross section per atom varies linearly with Z, the number of electrons per atom. The cross section varies with energy in a rather complicated way, monotonically decreasing with increasing energy.

The scattered photons vary in energy depending on the incident photon energy and on the angle of scattering according to the following law

$$\alpha' = \frac{\alpha}{1 + \alpha(1 - \cos\theta)}, \tag{14}$$

where α = primary photon energy in units of the electron rest energy, mc^2, 0.51 Mev,

α' = scattered photon energy, same units,

θ = angle of scattering.

There are several things to note about this expression. If θ is small, $\cos\theta \sim 1$, and for not too large α, $\alpha' \sim \alpha$. That is, the higher energy scattered photons proceed in a nearly forward direction. If

$$\theta \sim \frac{\pi}{2}, \ \alpha' \sim \frac{\alpha}{1 + \alpha} < 1.$$

That is, regardless of the initial energy, a photon scattered at right angles will never have an energy greater than 0.51 Mev. Next consider the fraction of the energy which is carried off by the scattered photon,

$$\frac{\alpha'}{\alpha} = \frac{1}{1 + \alpha\,(1 - \cos\theta)} \quad . \tag{15}$$

This fraction is less the greater the initial energy, a redeeming feature of the process in shielding.

Pair Production. In this process a photon interacts with the coulomb field of nucleus (and much less frequently with that of an electron) to disappear and produce a pair of electrons, one of each charge polarity. The effect does not occur unless the photon has sufficient energy to create the pair, that is 2 mc^2 or 1.02 Mev. Above this threshold the cross section continually rises, slowly at first and sharply at a few Mev. It is the dominant process for high energy gamma rays in heavy materials.

Since the process involves the coulomb field strength, the cross section would be expected to increase with nuclear charge. Actually it varies with $Z^2 + Z$, where the first term accounts for the processes which take place in the field of the nucleus and the latter sums up those in the fields of the singly charged electrons, Z in number.

This process, like the photoelectric effect, can be treated as absorption, in spite of the radiation which comes from positron annihilation, since this is of comparatively low energy (usually two 0.51 Mev photons) and isotropic.

The Relative Importance of the Gamma Interaction Processes

Hydrogen. This element displays almost no photoelectric effect and very little pair production. The latter is an important contribution only above about 30 Mev, a very high energy for reactor shielding. On the other hand, it does, of course, show the Compton effect, being at least twice as effective as any other element for a given weight. The reason for this is simply that it has no nuclear neutrons, which add weight but do not contribute to Z, the nuclear charge. Remember that gamma cross sections are characterized by Z, not A. The reader is warned not to design a gamma shield of hydrogen. It is available in such poor densities even in Liquid form that it is never very suitable. Furthermore, the lack of photoelectric absorption would give rise to large buildup factors.

Other Light Elements. Oxygen, nitrogen, carbon, etc. show mostly compton effect from about 0.04 Mev to about 15 Mev. Below this range the photoelectric effect becomes dominant, and above it the pair production is most important.

For hydrogen as well as the other light elements, it is seen that the compton process is very dominant. The result of this fact is that they are in general poorer gamma shields, having a large fraction of scattered radiation. In certain geometries the radiation which is scattered through an appreciable angle is the most important component, as for example the radiation which turns a corner by scattering in sea water and thus avoids a shielding bulkhead. This effect is relatively much more important with low Z materials.

Heavy Elements. For the heavy elements pair production and photoelectric effect are much more important, as is to be expected from the cross-sectonal dependence on Z. Unfortunately, however, even for uranium there is a very important intermediate energy region in which the Compton process

dominates. It is half or more of the total cross section from about 0.8 Mev to about 4 Mev, constituting about 70% of the total at 2 Mev. In reactor shielding this is an important range and cannot be neglected. It is an especially important region in shielding, since the cross sections of the best gamma shields all reach a minimum near where the Compton process is dominant. For this reason the buildup factor for scattered radiation cannot be neglected even with the heaviest elements.

On the other hand, the heavier the element the smaller is this Compton-dominated region, the less is the domination, the lower is the energy at which the minimum occurs, and the higher is the cross section per unit weight (hydrogen excepted) at the minimum. Radiation scattered at an angle is also much less likely to be large enough to be important.

The elements between oxygen and uranium are intermediate in their attenuation characteristics. It is well to point out the energies at which the minima occur for a few of these

Table 7 - Minima in Total Gamma Cross Section

Element	E_{min}
Al	20 Mev
Fe	8 Mev
Pb	3.2 Mev
U	3.1 Mev

The total cross sections are shown in Figures 2 and 3, which are taken from Powell and Snyder's report ORNL-421.

UNCLASSIFIED
DWG. 7753B

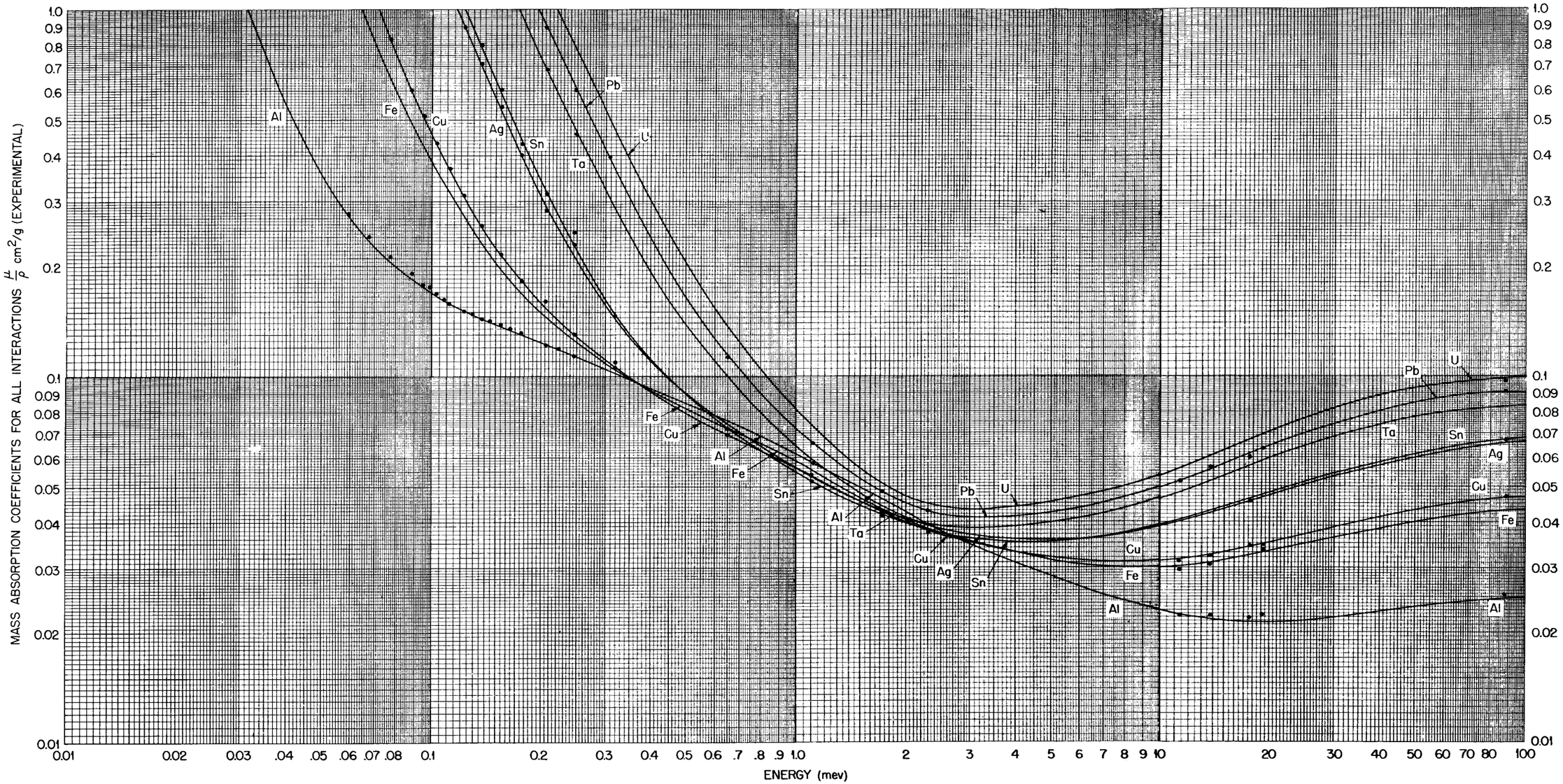

FIG. 2. MASS ABSORPTION COEFFICIENT FOR ALL INTERACTIONS $\frac{\mu}{\rho}$ VS ENERGY

(Macroscopic Total Cross-Section Divided by Density)

Supplement 1 to ORNL 421 "Absorption of γ-Rays" by Snyder and Powell

UNCLASSIFIED
DWG. 7754B

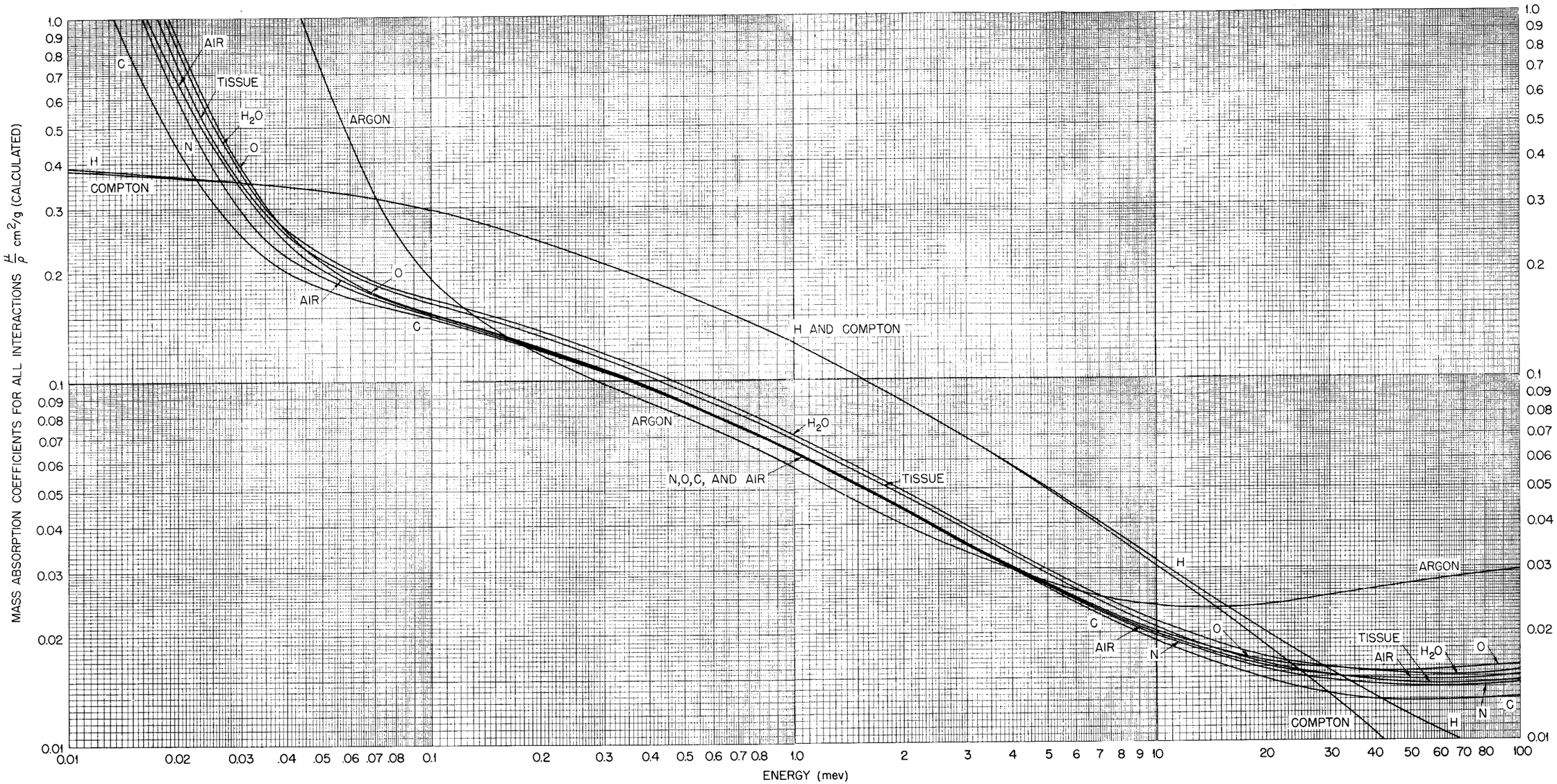

FIG. 3. MASS ABSORPTION COEFFICIENT FOR ALL INTERACTIONS $\frac{\mu}{\rho}$ VS ENERGY

(Macroscopic Total Cross-Section Divided by Density)

Supplement 2 to ORNL 421 "Absorption of γ-Rays" by Snyder and Powell

Gamma Energy-Absorption Cross Sections

In order to obtain the energy deposition from a flux of gamma rays, it is necessary to allow for that fraction of the energy which proceeds as gamma photons after Compton interaction. Of course to a good approximation the entire photon energy is deposited in the material on photoelectric or pair interaction. Figures 4 and 5, also taken from Powell and Snyder, show these cross sections. Their use is demonstrated in the following calculation of the relation between gamma flux and the physical unit of radiation, the Roentgen.

The Roentgen is defined as that quantity of electromagnetic (X- or gamma) radiation which produces ionization in 1 cubic centimeter of dry air at a standard temperature and pressure totalling one electrostatic unit of charge of each sign. Alternately it will dissipate 83 ergs per gram of wet tissue or 0.107 ergs per cubic centimeter of dry air. It is assumed that in the measurement the receptor is large enough so that the electrons produced by the gamma rays are stopped in it, while the secondary photons scattered in the Compton process are not. Of course no actual detector will satisfy these conditions exactly, but many approach them quite well. The edge effects for electrons are allowed for by utilizing the fact that all low-Z materials behave about the same in the interesting energy range in that they are predominantly Compton scatterers. With this assumption the Bragg-Gray principle[21] states that the ionization in a small gas-filled cavity will be the same as that within the body of the material corrected only for relative densities of gas and matrix material. Consequently if the ionization produced in a small air-filled cavity in some low-Z material (e.g. carbon) is measured, this will be an accurate indication of the ionization to be expected in a comparable volume without edge effects. Because of

UNCLASSIFIED
DWG. 8117 B

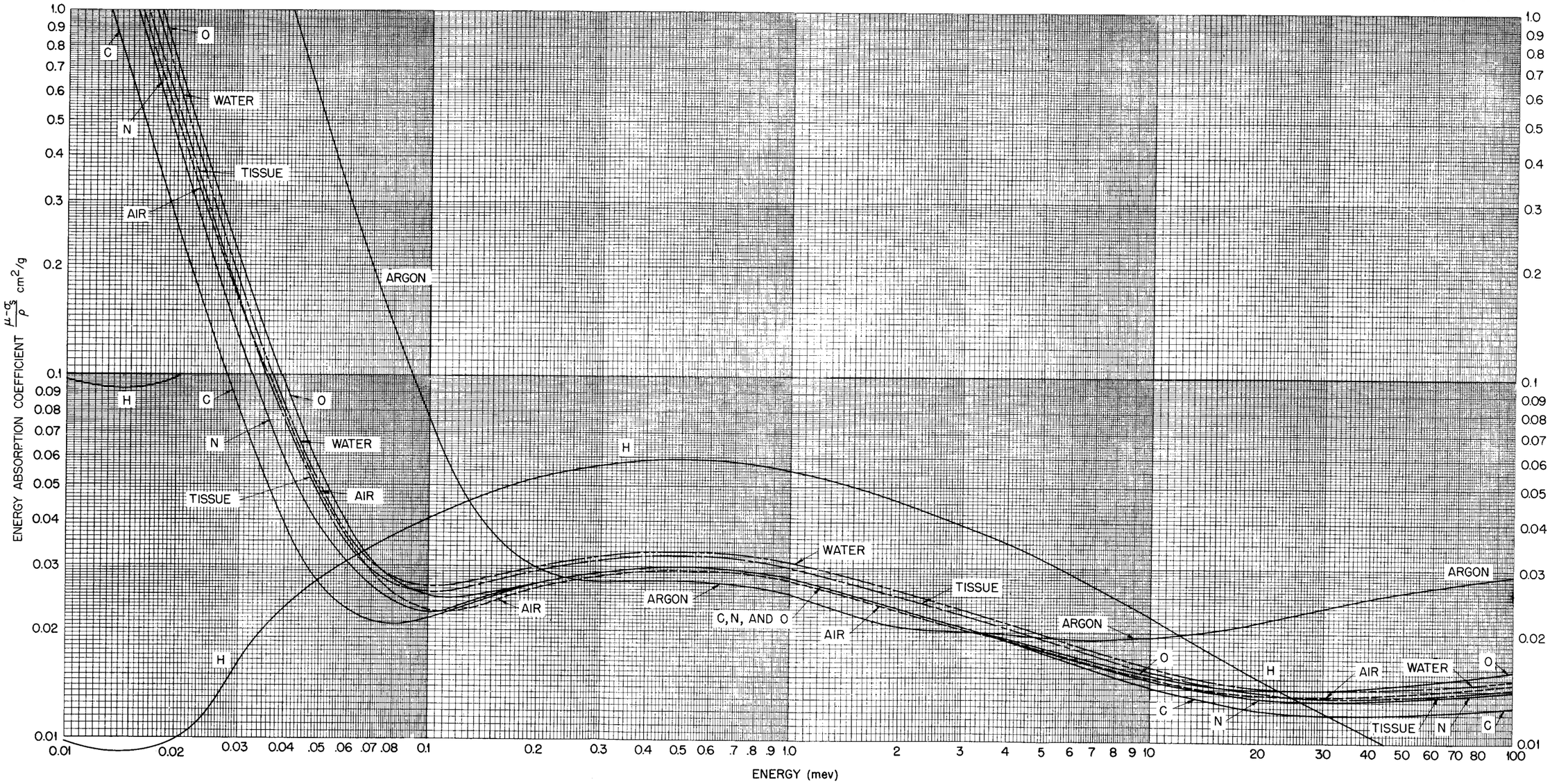

FIG. 4. MASS COEFFICIENT FOR ENERGY ABSORPTION $\frac{\mu-\sigma_s}{\rho}$ VS ENERGY

(Macroscopic Cross-Section for Energy Absorption Divided by Density)

Supplement 4 to ORNL 421 "Absorption of γ-Rays" by Snyder and Powell

UNCLASSIFIED
DWG. 8118B

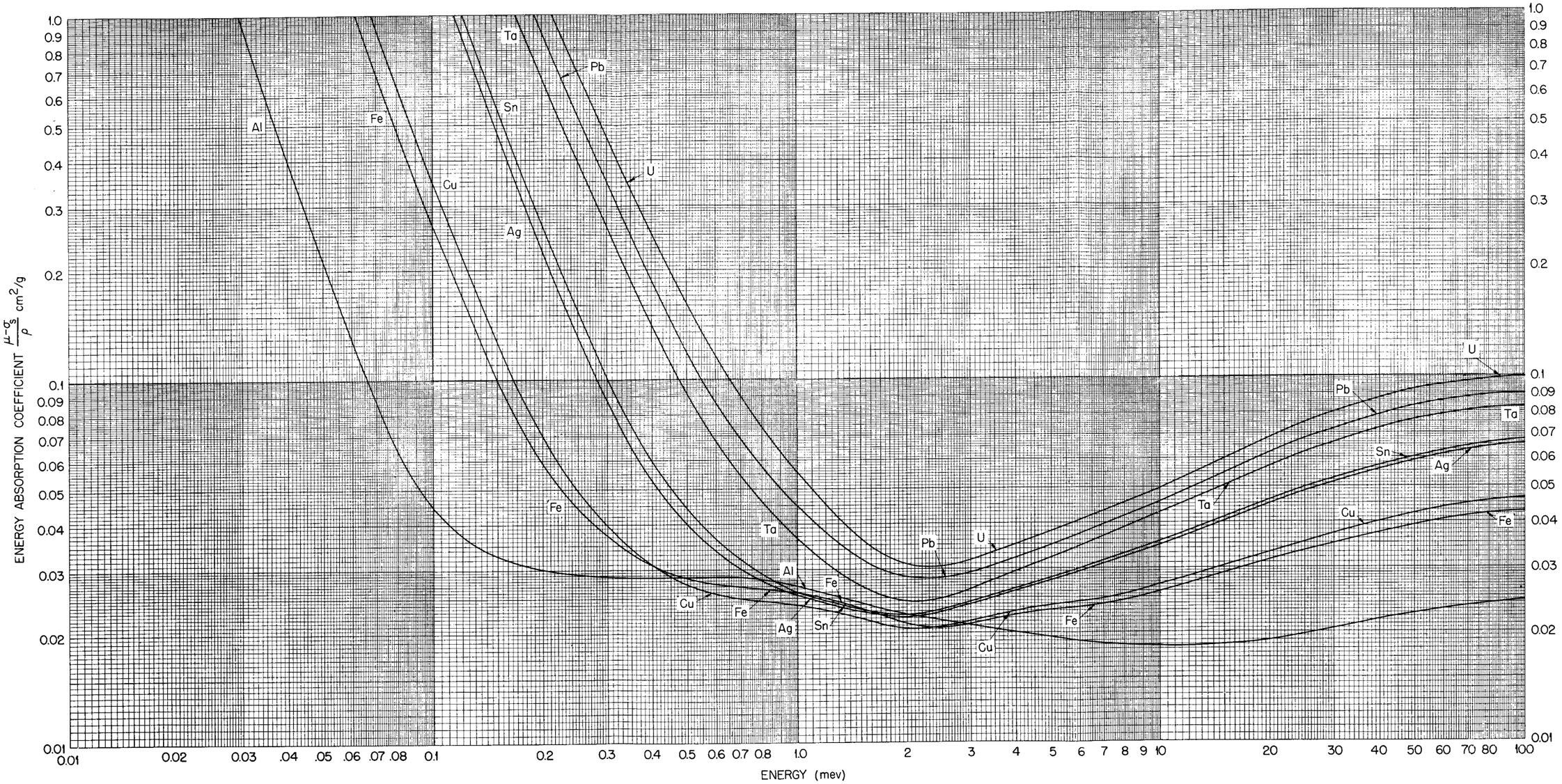

FIG. 5. MASS COEFFICIENT FOR ENERGY ABSORPTION $\frac{\mu-\sigma_s}{\rho}$ VS ENERGY

(Macroscopic Cross-Section for Energy Absorption Divided by Density)

Supplement 3 to ORNL 421 "Absorption of γ-Rays" by Snyder and Powell.

the great disparity between electron and photon ranges in the materials of construction, the wall thickness can be chosen thick with respect to the former and thin compared to the latter.

To illustrate the use of the energy-deposition data in Figures 4 and 5, let us now calculate the flux of 2 Mev gamma photons which corresponds to 1 R/hr.

$\Phi(E)$ = gamma flux, photons of energy E, per cm^2 sec,

$\mu_a(E)$ = energy absorption coefficient for photons of energy E in air, cm^{-1},

= 2.9×10^{-5} for E = 2 Mev

1.6×10^{-6} ergs X 1 Mev,

3600 seconds per hour,

$$1 \text{ R/hr} = \frac{0.107 \text{ ergs/cm}^3}{3600 \text{ sec}}$$

$$= 2 \text{ Mev} \times 1.6 \times 10^{-6} \text{ (ergs/Mev)} \times 2.9 \times 10^{-5} \text{ cm}^{-1} \times \Phi(2) \text{ cm}^{-2} \text{ sec}^{-1},$$

$$\Phi(2)(1 \text{ R/hr}) = 3.2 \times 10^5 \text{ 2 Mev photons cm}^{-2} \text{ sec}^{-1}.$$

The fluxes for 1 R/hr from other photon energies are shown in Figure 6.

GEOMETRY OF SHIELDING[22-24]

The Simple Geometries

In this section account is taken of the fact that most shielding calculations deal with distributions of sources and attenuators. The relations between some of the more common situations and the basic geometry are developed.

Plane Collimated Source. This has already been treated in the section on cross sections. The fundamental law is the exponential,

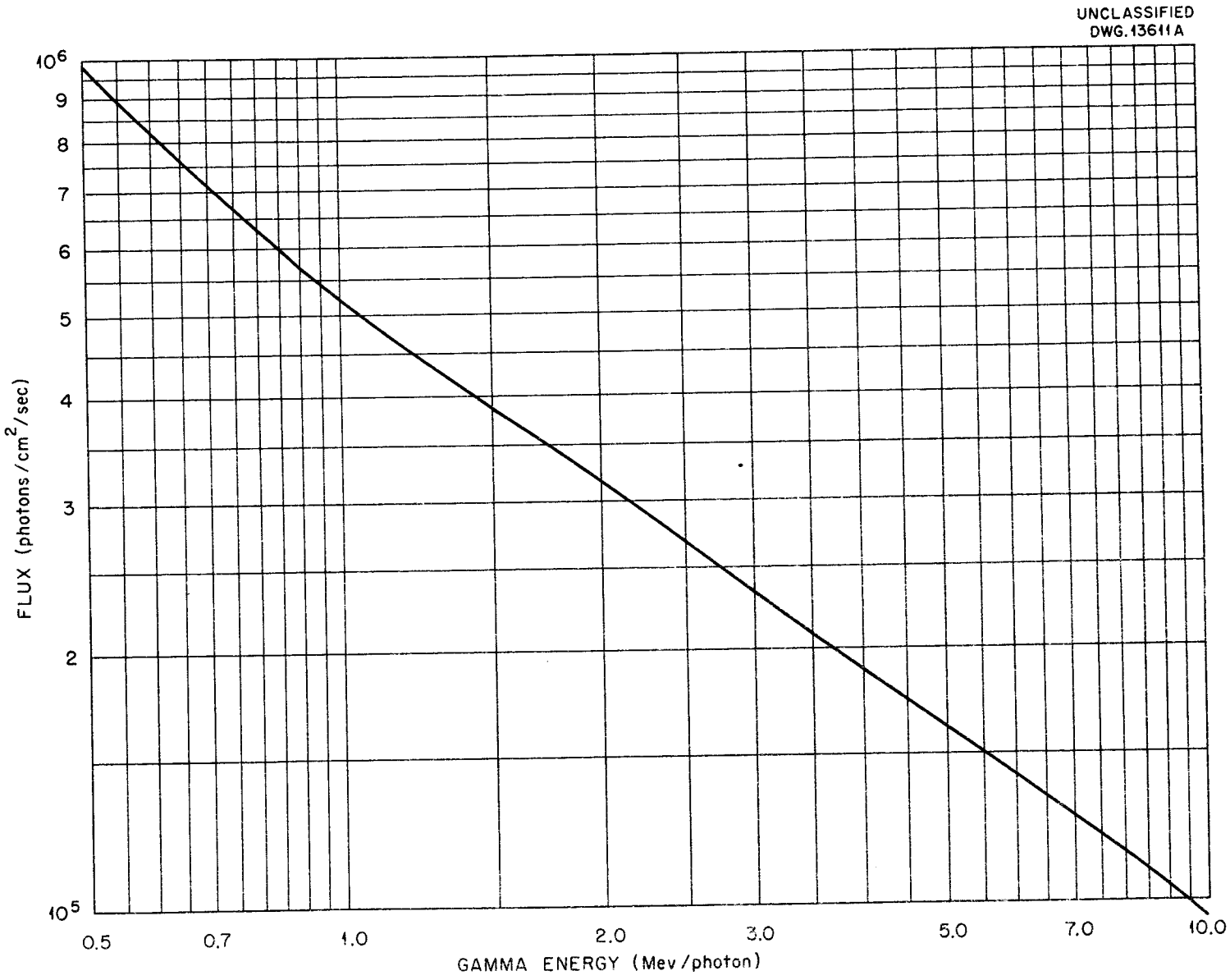

Fig. 6. Gamma Flux for One Roentgen per Hour.

$$I(z) = I(0)\, e^{-z/\lambda}, \tag{16}$$

$I(z)$ = intensity or flux at z, $cm^2\ sec^{-1}$, collimated along Z,

λ = relaxation length of shielding material,

or λ = reciprocal of μ, the absorption coefficient,

or λ = reciprocal of macroscopic cross section, Σ,

if $I(z)$ refers to uncollided flux.

Inverse Square Law.

$$I(r) = \frac{S}{4\pi r^2} \tag{17}$$

$I(r)$ = intensity, particles $cm^{-2}\ sec^{-1}$, at distance r from source, no shield.

S = strength of point source, particles per second

Point Source and Spherical Shield. In case a spherical shell shield is interposed between source and receptor,

$$I(r) = \frac{S\, e^{-(r_1 - r_o)/\lambda}}{4\pi r^2} \tag{18}$$

r_o = inner radius of shield

r_1 = outer radius of shield

r = distance from source to detector.

In the case of a source imbedded in a medium, $r_o = 0$.

For several successive layers of shielding, the simple expression becomes

$$I(r) = S\, e^{-\left\{\frac{r_1 - r_o}{\lambda_1} + \frac{r_2 - r_1}{\lambda_2}\right\}} \tag{19}$$

Type of Detector

With a single point source or a collimated source, and no deflections due to scattering, it is unnecessary to specify the shape of detector. When, however, radiation arrives from many directions, this ambiguity is no longer tolerable. Accordingly the two types of most use are now defined. It should be pointed out that the detectors to be described are not those such as might be used in an experiment, but rather hypothetical pure types for which calculations can be made. Most actual detectors, including the human body, resemble both types to some extent, but usually one more than the other.

Directional Detector. This detector can be characterized by a small flat black body which records the total number or intensity of arrivals on its surface and is, unless otherwise specified, assumed to be perpendicular to the preferred direction of propagation. Thus the response is proportional to the cosine of the angle between actual arrival and the preferred direction.

It is this type of detector which is to be used in calculating the total leakage from a surface, or the total arrivals at a surface, either of which could be used to specify a second soruce, say due to neutron captures. It is approached experimentally by a foil so thick that essentially all incident neutrons record. The reading on this detector will in general be indicated by J, implying a radiation current.

Isotropic Detector. The isotropic detector is characterized by a small black sphere, which of course presents the same target size to all directions. This detector is sometimes referred to as a "milligoat" since a small meatball would presumably serve as a useful detector if the dosage in it could be recorded. It is obvious that this detector will always record

an intensity of radiation at least as high as that recorded on the directional detector, and hence the milligoat reading gives the maximum rate of radiation reception by, for example, the human body. It should be used, therefore, whenever the radiation is not definitely collimated. It can always be used for an upper limit, which gives of course a conservative shield design. The response of this detector will in general be indicated by D, implying a dose rate. The area by which the rate of arrivals must be divided to obtain flux is that of a great circle of the sphere. (Radius = $1/\sqrt{\pi}$).

General Transformations for Unspecified Attenuation Functions

In shielding theories, attenuation is usually expressed in terms of either a point source or an infinite plane collimated source in an infinite medium. Most shielding meaurements have been made with a uniform disc source in a "semi-infinite" medium. Most reactors, on the other hand, approximate cubes, cylinders, or spheres. In order to convert from one shape to another certain geometrical manipulations are used which will presently be demonstrated.

The Point-to-Point Attenuation Kernel

For the purpose of calculating the intensity in other geometries, a function G(R) is used, which is defined as the response of a detector at a distance R in the shield from a unit source. G(R) is of course characteristic of the source, the detector, and the medium. Thus the source might be a gamma emitter, the medium water, and the detector an ionization chamber. The source must be isotropic, the detector non-directional, and the medium must attenuate the same for all distances R regardless of position or direction. Thus, for a point source of strength S a distance R from an isotropic detector,

$$D_{Pt}(R) = S\,G(R). \tag{20}$$

Of course the conditions imposed on G(R) are never exactly satisfied in experiment or installation, but usually, on the other hand, it is a good approximation to use the results derived with the aid of the ideal function. Some of the conditions which make G(R) not a unique function of R are the following:

a. The source itself is not infinitely small or thin and consequently absorbs some of its own radiation, leaving the remainder not isotropic. This absorption is not always comparable to that of the shield material displaced.

b. The "medium" seldom is present on both sides of a plane source, as is required in the assumption.

c. Not only does the medium terminate before infinity - it usually cuts off just at the measuring point so that the effect may in some cases be appreciable.

d. Many shields are laminated so that the properties of the medium are not isotropic, that is, they do not attenuate at the same rate for all directions. This can be especially true for gamma rays.

e. Reactors are of considerable size, hence are often treated as if the surface were a thin isotropic source and the volume is counted as shielding medium. Both assumptions are obviously incorrect, but the inaccuracies they introduce are usually not excessive. Treatment of reactor material as if it were shielding is not a bad approximation, since after all the purpose of most of the material is to "contain" the neutrons, i.e., to attenuate the fast neutrons.

<u>Plane Isotropic Source in Infinite Medium.</u> In this case the source is assumed infinitely thin, all in one plane, of uniform strength σ particles emitted isotropically per unit area of source per unit time, and imbedded in

an infinite medium. The response of the isotropic detector at a distance away from the infinite source, $D_{Pt}(z,\infty)$, is now calculated

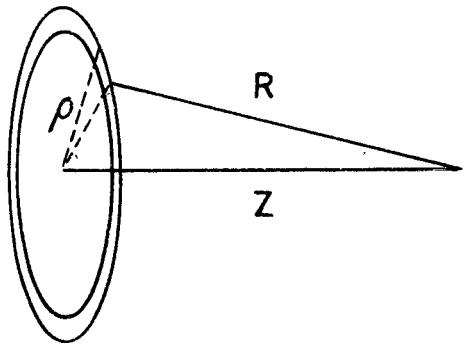

Figure 7

$$D_{P\ell}(z,\infty) = \int_{\rho=0}^{\infty} 2\pi\rho \, d\rho \, \sigma \, G(R)$$

$$R^2 = \rho^2 + z^2$$

$$2R \, dR = 2\rho \, d\rho$$

$$D_{P\ell}(z,\infty) = 2\pi\sigma \int_{z}^{\infty} G(R) \, R \, dR. \tag{21}$$

The relation between point and plane source geometries is obtained by differentiating (21)

$$\frac{d}{dz} D_{P\ell}(Z,\infty) = -2\pi \, \sigma z \, G(z) \tag{22}$$

$$\frac{d}{dz} D_{P\ell}(Z,\infty) = -2\pi \frac{\sigma}{S} z D_{Pt}(z) \quad . \tag{23}$$

In case the plane source is confined to a disc of radius "a" and the detector is on the axis of the source,

$$D_{P\ell}(z,a) = \int_{\rho=0}^{\rho=a} 2\pi\sigma\rho \, d\rho \, G(R)$$

$$= 2\pi\sigma \int_{z}^{\sqrt{z^2+a^2}} G(R) \, R \, dR$$

Since much of the experimental work on shielding has been carried out with a disc source, it is important to investigate a method of obtaining more fundamental information from the observed data. That is, it is desirable to find the point to point kernel from data taken at points on the axis of a disc source. For this purpose, Eq. (24) is differentiated. Thus

$$D'_{P\ell}(z,a) = 2\pi\sigma \left[G(\sqrt{z^2+a^2}) \sqrt{z^2+a^2} \frac{d}{dz} \sqrt{z^2+a^2} - G(z) \, z \right]$$

$$\frac{D'_{P\ell}(z,a)}{2\pi\sigma z} = G(\sqrt{z^2+a^2}) - G(z) \, . \tag{25}$$

Defining

$$B(z) = -\frac{D'_{P\ell}(z,a)}{2\pi\sigma z} ,$$

it is found, using the recursion formula (25), that

$$G(z) = B(z) + B(\sqrt{z^2+a^2}) + B(\sqrt{z^2+2a^2}) + \ldots \tag{26}$$

$$= \sum_{\nu=0}^{\infty} B(\sqrt{z^2+\nu a^2})$$

The last equation defines a method of determining the kernel from the data using straight forward operations. It is only applicable for "a" large compared to the attenuation length of the radiation, but for those cases in which this condition is not met the disc will be a good approximation to a point source and the data will indicate G(R) directly.

Problem 1.

Suppose that the disc source shrinks so that $a \to 0$, but subject to the constraint that $\pi a^2 \sigma = S$. This should lead to the case of a point source. Show how (20) can be derived from (24) for this situation.

Hurwitz of Knolls Atomic Power Laboratory has pointed out that if the dose from a finite disc source is known as a function of distance along the axis, then the dose to be expected from an infinite source is also known. The Hurwitz expression is as follows

$$D_{P\ell}(Z,\infty) = D_{P\ell}(Z,a) + D_{P\ell}(\sqrt{Z^2 + a^2},a) + D_{P\ell}(\sqrt{Z^2 + 2a^2},a) + \ldots$$

$$= \sum_{\nu=0}^{\infty} D_{P\ell}(\sqrt{Z^2 + \nu a^2},a) \qquad (27)$$

This is verified by substituting (24) in (27) to obtain the following identity*

$$\int_Z^{\infty} = \int_Z^{\sqrt{Z^2 + a^2}} + \int_{\sqrt{Z^2 + a^2}}^{\sqrt{Z^2 + 2a^2}} + \int_{\sqrt{Z^2 + 2a^2}}^{\sqrt{Z^2 + 3a^2}} + \ldots$$

---

*Note that from (24) we have:

$$D_{P\ell}(\sqrt{Z^2 + \nu a^2},a) = 2\pi\sigma \int_{\sqrt{Z^2 + \nu a^2}}^{\sqrt{Z^2 + (\nu + 1)a^2}} G(R)\, R\, dR$$

Of course for (27) to be useful the series must converge quickly. It is seen that this will be the case for "a" large compared to the relaxation length of the radiation, as is to be expected since the larger is $\frac{a}{\lambda}$ the more nearly the source appears to be infinite in extent. Note that the Hurwitz transformation, represented by (27), gives an accurate method for estimating the intensity which would be expected from a source infinite in extent on the basis of data taken with a finite source. The method for finding the infinite source reading at a point Z centimeters away is simply to add the measured intensities for a source of radius a at points on its axis at distances of $Z, \sqrt{Z^2 + a^2}, \sqrt{Z^2 + 2a^2}, \sqrt{Z^2 + 3a^2}, + \ldots$ etc. This is the preferred method.

There are situations in which the preferred method is not applicable. For example, the intensity may have been so low that the last point of interest is also the most distant one which could be measured. In this case it may be permissible to calculate the correction according to the following approximate method.

If the data for a finite disc of radius "a" can be expressed in the region of interest by a simple exponential of relaxation length λ, then

$$1 + \alpha > \frac{D_{P\ell}(Z,\infty)}{D_{P\ell}(Z,a)} \gtrsim \frac{1}{2} + \alpha \tag{28}$$

$$\alpha = \frac{2\lambda^2}{a^2}\left(\frac{Z}{\lambda} + 1\right) \tag{29}$$

The proof of (28) proceeds as follows.

If the data is representable by a simple exponential, then the intensity at $\sqrt{Z^2 + a^2}$ will be lower than that at Z by the factor $e^{-\frac{1}{\lambda}(\sqrt{Z^2 + a^2} - Z)}$. That is

$$D_{P\ell}(\sqrt{Z^2 + a^2}, a) = D_{P\ell}(Z,a)\, e^{-\frac{1}{\lambda}(Z - \sqrt{Z^2 + a^2})} . \tag{30}$$

Putting this expression into the Hurwitz equation,

$$D(Z,\infty) = D(Z,a)\, e^{Z/\lambda} \sum_{\nu=0}^{\infty} e^{-\sqrt{Z^2 + \nu a^2}/\lambda} \tag{31}$$

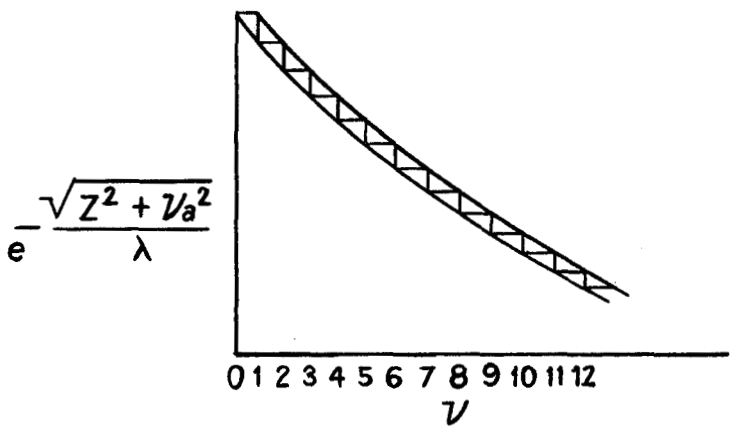

Figure 8

In Figure 8 the summation is represented by the steps. The area under the lower curve, which is obtainable by quadrature, represents a lower bound. This lower curve has been moved to the right one unit and redrawn to demonstrate that the lower bound plus the first term $e^{-Z/\lambda}$ represents an upper bound.

$$U > \sum_{\nu=0}^{\infty} e^{-(\sqrt{Z^2 + \nu a^2})/\lambda} > L$$

$$U = L + e^{-Z/\lambda} .$$

The lower bound is found as follows

$$L = \int_{\nu=0}^{\infty} e^{-(\sqrt{Z^2 + \nu a^2})/\lambda} d\nu$$

$$= 2\left(\frac{\lambda}{a}\right)^2 \int_{Z/\lambda}^{\infty} e^{-y} y dy$$

$$= 2\left(\frac{\lambda}{a}\right)^2 \left(\frac{Z}{\lambda} + 1\right) e^{-Z/\lambda} \tag{32}$$

To find whether the arithmetic mean of the two bounds L and U is itself an upper or lower bound, we investigate the curvature of the expression

$$b(\nu) = e^{-\sqrt{Z^2 + \nu a^2}/\lambda}$$

$$\frac{d^2b}{d\nu^2} = \left(\frac{a^4}{4\lambda^2(Z^2 + \nu a^2)} + \frac{a^4}{4\lambda(Z^2 + \nu a^2)^{3/2}}\right) e^{-\sqrt{Z^2 + \nu a^2}/\lambda} .$$

For positive ν and λ, $\frac{d^2b}{d\nu^2}$ is positive, so that the arithmetic mean of L and U must itself represent a lower limit to the sum. Consequently

$$U > \sum_{\nu=0}^{\infty} e^{-(\sqrt{Z^2 + \nu a^2})/\lambda} > L' > L \tag{33}$$

where

$$L' = \frac{1}{2}(L + U) = L + \frac{1}{2} e^{-Z/\lambda} \tag{34}$$

Substitution of (32), (33) and (34) in (31) yields (28) and (29). It is further to be noted that the lower limit in (28) is probably the closer estimate of the true value of the ratio.

Plane to Sphere Transformation. It is often of interest to calculate the intensity to be expected from a source spread uniformly over the surface of a sphere. The usual isotropic medium is assumed, and this must extend inside as well as outside the sphere. The geometry is shown in Figure 9.

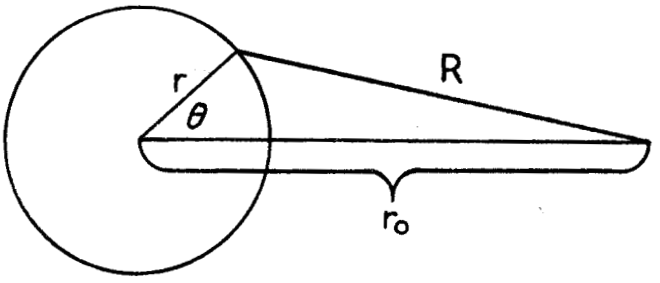

Figure 9

For this case

$$D_S(r_o,r) = 2\pi\sigma r^2 \int_{\theta=0}^{\pi} G(R) \sin\theta \, d\theta$$

$$R^2 = r^2 + r_o^2 - 2rr_o \cos\theta,$$

$$2R \, dR = 2rr_o \sin\theta \, d\theta,$$

$$D_S(r_o,r) = 2\pi\sigma \frac{r}{r_o} \int_{r_o - r}^{r_o + r} G(R) \, R \, dR$$

$$= \frac{r}{r_o} \left\{ 2\pi\sigma \int_{r_o - r}^{\infty} G(R) \, R \, dR - 2\pi\sigma \int_{r_o + r}^{\infty} G(R) \, R \, dR \right\}$$

$$= \frac{r}{r_o} \left\{ D_{P\ell}(r_o - r, \infty) - D_{P\ell}(r_o + r, \infty) \right\} . \tag{35}$$

Problem 2.

As $r \to 0$, expression (35) must approach that for a point source with strength $S = 4\pi r^2 \sigma$. Show this.

If $2r \gg \lambda$, the relaxation length, then the second term in the bracket will be negligible compared to the first, and the following approximate expression becomes useful

$$D_S(r_o, r) \cong \frac{r}{r_o} D_{P\ell}(r_o - r, \infty) \quad . \tag{36}$$

<u>Example.</u> Suppose it is desired to find the intensity of radiation outside a 120 cm thick shield surrounding a 60 cm radius spherical reactor. The effective source strength of the reactor surface is 3×10^{14} neutrons/cm^2/sec.

Data on which to base the design: A disc source of radius 30 cm and of surface strength 2.5×10^7 neutrons/cm^2/sec yields an intensity of 2.5×10^3 n/cm^2/sec at a thickness of 120 cm of the same shielding material. At this distance, the apparent relaxation length of the radiation was 9 cm.

Solution

$$D_{P\ell}(120,30) = 2.5 \times 10^3 \text{ for } \sigma = 2.5 \times 10^7.$$

Hurwitz correction, h:

$$h = \frac{1}{2} + \alpha = \frac{1}{2} + \frac{2 \cdot 9^2}{30^2}\left(\frac{120}{9} + 1\right) = 3.08$$

$$D_{P\ell}(120,\infty) = 3.08\, D_{P\ell}(120,30) = 7.7 \times 10^3 \text{ for } 6 = 2.5 \times 10^7 \ .$$

For $\sigma = 3 \times 10^{14}$,

$$D_{P\ell}(120,\infty) \cong 7.7 \times 10^3 \times \frac{3 \times 10^{14}}{2.5 \times 10^7} \cong 9.24 \times 10^{10} \text{ n/cm}^2\text{/sec} \quad .$$

Using (33)

$$D_S(180,60) = \frac{60}{120 + 60} \times 9.24 \times 10^{10} \text{ n/cm}^2\text{/sec} = 3.08 \times 10^{10} \text{ n/cm}^2\text{/sec} \ .$$

Plane to Cylinder Transformation. There is no simple general transformation for this case, but it can be shown for most specific attenuation kernels that the relation between cylindrical and plane geometry for large attenuations (thick shields) should be approximately

$$D_C(r_o,r) \cong \sqrt{\frac{r}{r_o}}\, D_{P\ell}(r_o - r, \infty), \tag{37}$$

where

$D_C(r_o,r)$ is the dose to be expected from an infinitely long cylindrical source of surface strength σ imbedded in shielding material,

r_o is the distance from the axis to the measuring point,

r is the cylinder radius,

$D_{P\ell}(r_o - r, \infty)$ is the dose to be expected at a distance $r_o - r$ from an infinite plane source of surface strength σ, imbedded in the same shielding material.

This relation (37) is not unreasonable, in that the cylinders intermediate between plane and sphere, and the factor of proportionality, $\sqrt{r/r_o}$, is intermediate between unity and that for plane to sphere, Eq. (36).

There remains the problem of correcting for the fact that the cylinder is not infinite in length. This is not, however, very important in most shields, and an approximate correction is adequate. For this purpose one can use certain upper bounds. A cylinder of length ℓ and diameter no greater than ℓ will in no case give more dose than a disc of radius ℓ, for example.

There is correspondingly no simple method of estimating the dose as a function of vertical distance from the cylinder midplane. Again, however, an upper estimate is available. At the end planes the dose is no greater than one half of that due to an infinite cylinder. In general it is simplest and safest to neglect the finiteness of the cylinder, unless it is very short in comparison with the distance from detector to the nearest part of the cylinder.

In case the cylinder is short in comparison with the shortest path from cylinder to detector, or more particularly if

$$\sqrt{\left(\frac{H}{2}\right)^2 + (r_o - r)^2} - (r_o - r) \leqq \lambda, \tag{38}$$

where

H = cylinder height,

λ = relaxation length for $G(R)$,

which means that the radiation from the end of the cylinder is nearly as effective (within a factor of e) as that from the mid-plane, then the cylinder can be approximated by a circular loop.

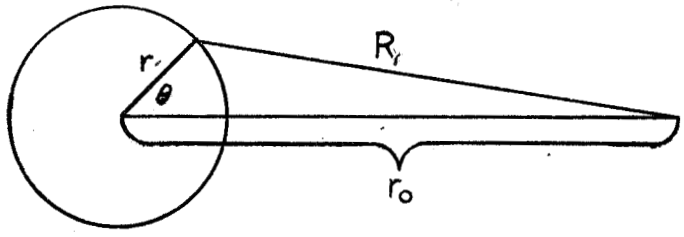

Figure 10

If the source strength per circumferential unit distance is s, $(s = h\sigma)$, then

$$D_\ell(r_o, r) = 2sr \int_{\theta=0}^{\pi} G(R)\, d\theta = 4sr \int_{r_o - r}^{r_o + r} \frac{G(R)\, R\, dR}{\sqrt{4r^2 r_o^2 - (R^2 - r^2 - r_o^2)^2}} \tag{39}$$

$G(R)$ can be had from experimental data via equation(22) and then (39) can be evaluated, numerically if necessary.

Although it is possible to extend the treatment of transformations somewhat further without specifying the form of the attenuation kernel, nevertheless it is usually much easier to choose some simple form which will fit at least over a limited range and to use this in the transformations. The next section demonstrates this method.

Geometry for Partially Specified Attenuation Functions.

In this section advantage will be taken of the fact that the attenuation in shields is large, so that contributions from the nearest sources are dominant and crude approximations are adequate to indicate the additional contributions of more distant courses. This process is commonly used in shielding with considerable success.

Consider an isotropic source spread uniformly over a curving surface so that the strength of the source on an element of area dS is just σdS. Let the nearest source point be located at the origin, the surface being tangent to the xy plane at the origin and then curving away so that the distance between the surface and the xy plane is given approximately by

$$z_1 = \frac{1}{2}\left(\frac{x^2}{a} + \frac{y^2}{b}\right). \tag{40}$$

Thus "a" and "b" are normal curvatures of the surface, and use of Eq. (40) is a direct consequence of the assumption regarding distant sources, since it surely will not fit well except in the region near the origin.

The detector is at z, and the distance from this to the element of surface dS is R.

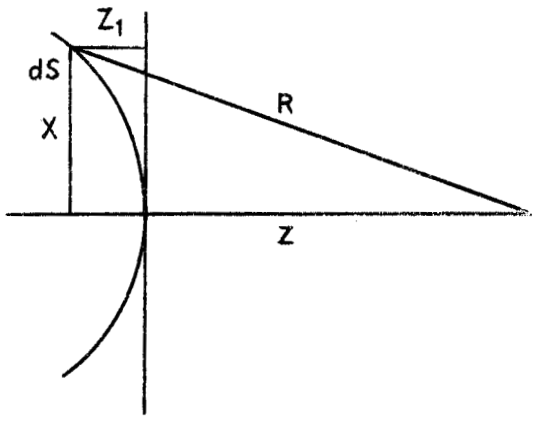

Figure 11

The reading on a milligoat detector is then

$$D(z) = \sigma \int_{\text{surface}} G(R)\, dS, \tag{41}$$

$$dS = dx\, dy \sqrt{1 + \left(\frac{\partial z_1}{\partial x}\right)^2 + \left(\frac{\partial^2 1}{\partial y}\right)^2} \cong dx\, dy \left(1 + \frac{x^2}{2a^2} + \frac{y^2}{2b^2}\right) \tag{42}$$

G(R) is now approximated by an unspecified (and therefore presumably exact) function for the kernel for the distance z, times an exponential for the extra distance (r - z).

$$G(R) \cong G(z)\, e^{-(R - z)/\lambda} \tag{43}$$

λ is a relaxation length, presumably one which makes Eq. (43) correct. Actually, since λ will be slowly varying, it can be taken from almost any convenient data for the proper material and source with attenuation over a distance of about z. For example, λ could be taken directly from Lid Tank data.

An approximate form is now required for R in order to make Eq. (41) integrable,

$$R = \sqrt{(z_1 + z)^2 + x^2 + y^2} \quad . \tag{44}$$

On expanding and ignoring terms of the order of z_1^2, in comparison with x^2 and y^2, it is found that

$$R - z \cong \frac{x^2}{2z} + \frac{y^2}{2z} + \frac{x^2}{2a} + \frac{y^2}{2b} \quad . \tag{45}$$

If Eq. (45) is accepted as adequate,

$$D(z) = \sigma\, G(z) \int_{-\infty}^{\infty} dy \int_{-\infty}^{\infty} dx\, e^{-\left[\frac{x^2 + y^2}{2\lambda z} + \frac{x^2}{2\lambda a} + \frac{y^2}{2\lambda b}\right]} \left[1 + \frac{x^2}{2a^2} + \frac{y^2}{2b^2}\right] \tag{46}$$

A cumbersome but not difficult integration yields

$$D(z) \cong 2\pi\sigma\, G(z) \left\{ \frac{1}{\left(\frac{1}{\lambda z} + \frac{1}{\lambda a}\right)^{1/2} \left(\frac{1}{\lambda z} + \frac{1}{\lambda b}\right)^{1/2}} + \frac{1}{2a^2 \left(\frac{1}{\lambda z} + \frac{1}{\lambda a}\right)^{3/2} \left(\frac{1}{\lambda z} + \frac{1}{\lambda b}\right)^{1/2}} + \frac{1}{2b^2 \left(\frac{1}{\lambda z} + \frac{1}{\lambda a}\right)^{1/2} \left(\frac{1}{\lambda z} + \frac{1}{\lambda b}\right)^{3/2}} \right\} \tag{47}$$

The last two quantities in the braces are in general much smaller than the first for a and b large compared to λ.

$$D(z) \approx 2\pi\sigma\, G(z) \left[\frac{1}{\left(\frac{1}{\lambda z} + \frac{1}{\lambda a}\right)^{1/2} \left(\frac{1}{\lambda z} + \frac{1}{\lambda b}\right)^{1/2}} \right] \tag{48}$$

for a, b $\gg \lambda$.

For a sphere $a = b = r$,

$$z = r_o - r$$

$$D_S(r_o, r) = 2\pi\sigma\, G(z)\, \lambda z\, \frac{r}{r_o} \quad . \tag{49}$$

If at this point it is recognized that

$$\frac{d}{dz} D_{P\ell}(z,\infty) = \frac{D_{P\ell}(z,\infty)}{\lambda} \tag{50}$$

then it is possible at once to confirm that Eqs. (49) and (36) agree.

For a cylinder, $a = \infty$, $b = r$, and $z = r_o - r$. By similar manipulation it is seen that Eq. (48) then confirms Eq. (37).

Geometry for the Simple Attenuation Functions

In this section two forms for the general function G(R) are assumed, viz:

(A) Exponential attenuation:

$$G_A(R) = \frac{e^{-\mu R}}{4\pi R^2} \tag{51}$$

(B) Exponential attenuation with linear buildup factor:

$$G_B(R) = B(R)\, G_A(R) \tag{52}$$

$$B(R) = \mu R \quad (\mu R \gg 1) \tag{53}$$

$$G_B(R) = \frac{\mu e^{-\mu R}}{4\pi R} \tag{54}$$

The same two detectors will be used as in the previous section, viz.:

a) Directional detector, flat, black, perpendicular to preferred direction, unit area. Response designated by J.

b) Isotropic detector, spherical, black, unit cross sectional area, (radius = $1/\sqrt{\pi}$), here referred to as the milligoat. Response designated by D.

Slab Geometry

Of considerable interest is the so-called slab shield, that is, one bounded by two parallel planes. It is assumed large (essentially infinite) in the other dimensions in comparison with its thickness, so that edge

effects are negligible. In this geometry it will be convenient to refer to the tabulated function $E_n(x)$, exponential integral function, which is defined as follows:

$$E_n(x) = \int_x^\infty \frac{e^{-p}}{p^n} \, d\,p \, . \tag{55}$$

An approximation for large values of x can be had by integration by parts:

$$\int_x^\infty \frac{e^{-p}}{p^n} \, d\,p = - \frac{e^{-p}}{p^n}\Bigg]_x^\infty - n \int_x^\infty \frac{e^{-p}}{p^{n+1}} \, d\,p \tag{56}$$

$$\approx \frac{e^{-x}}{x^n} \text{ for large } x \tag{57}$$

a) Isotropic Plane Source. The simplest source to be treated is assumed to be in a plane, to be so thin that there is no absorption within the source, to be of uniform surface strength, σ cm^{-2} sec^{-1}, and to be isotropic, so that the emission into solid angle is $\sigma/4\pi$ cm^{-2} sec^{-1}.

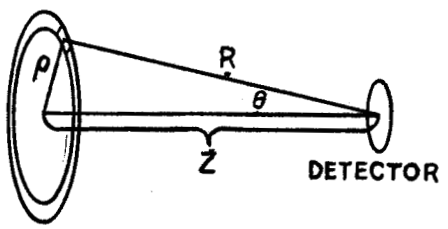

Figure 12

Exponential Attenuation, Directional Detector.

$$J_A(Z) = 2\pi\sigma \int_{\rho=0}^{\infty} G_A(R)\, \rho d\rho \, \frac{Z}{R}$$

$$R^2 = \rho^2 + Z^2$$

$$2R\, dR = 2\rho d\rho$$

$$J_{A1}(Z) = 2\pi\sigma \int_{Z}^{\infty} \frac{e^{-\mu R}}{4\pi R^2} \frac{Z}{R}\, R\, d\, R = \frac{\sigma Z\mu}{2} \int_{\mu Z}^{\infty} \frac{e^{-x}dx}{x^2} = \frac{\sigma Z\mu}{2}\, E_2(\mu Z) \tag{58}$$

$$\approx \frac{\sigma}{2} \frac{e^{-\mu Z}}{\mu Z} \text{ for large } \mu Z \tag{59}$$

Exponential Attenuation, Milligoat Detector.

$$D_{A1}(Z) = 2\pi\sigma \int_{\rho=0}^{\infty} G(R)\, \rho d\rho \tag{60}$$

$$= \frac{\sigma}{2} E_1\, (\mu\, Z) \tag{60}$$

$$\approx \frac{\sigma}{2} \frac{e^{-\mu Z}}{\mu Z} \tag{61}$$

Linear Buildup, Directional Detector.

$$J_{B1}(Z) = 2\pi\sigma \int_{\rho=0}^{\infty} G(R)B(R)\, \frac{Z}{R}\, \rho d\rho$$

$$= \frac{\sigma Z}{2} \int_{Z}^{\infty} \frac{e^{-\mu R}}{R^2} \frac{\mu R}{R}\, RdR = \frac{\sigma Z\mu}{2}\, E_1\, (\mu Z) \tag{62}$$

$$J_{B1}(Z) \approx \frac{\sigma e^{-\mu Z}}{2} \tag{63}$$

Problem 3.

Show that $D_{B1} = \frac{\sigma}{2} e^{-\mu Z}$. (64)

---

b) Shielded Semi-infinite Volume-distributed Source. In this section we consider the case of a source which is very thick, so that the self-absorption is important. The specific activity of the source is designated by $A, cm^{-3}\ sec^{-1}$. An example of this case is the sodium coolant from a reactor. This might for example be present in large volumes outside the reactor, and it would be necessary to calculate the dose, both directly adjacent to the bare source, and at some position behind a slab shield. The self-absorption in the sodium could be treated adequately with either of the simple functions, $G_A(R)$ or $G_B(R)$. For this prupose we will use μ_1 for the characteristic attenuation coefficient for the source, retaining μ for the shield as heretofore.

We now calculate the dose at a depth Z in a shield which attenuates exponentially, and which is adjacent to a semi-infinite (plane-limited) self-absorbing source.

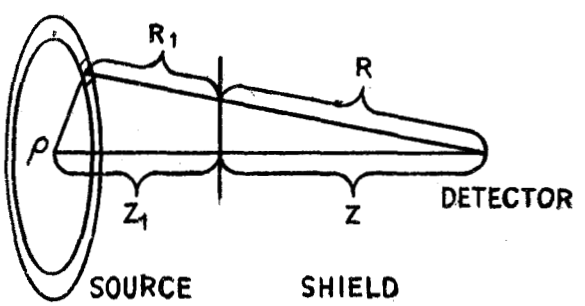

Figure 13

$$D_{A2}(Z) = \alpha \int_{\rho=0}^{\infty} \int_{Z_1=0}^{\infty} \frac{e^{-\mu_1 R_1 - \mu R}}{4\pi(R + R_1)^2} 2\pi \rho \, d\rho \, dZ_1$$

$$\rho^2 + (Z + Z_1)^2 = (R + R_1)^2$$

Since ρ and Z are independent,

$$2 \rho \, d\rho = 2(R + R_1) \, d(R + R_1) \, .$$

Furthermore,

$$\frac{R_1}{R} = \frac{Z_1}{Z}$$

so that

$$\mu_1 R_1 + \mu R = \left(\frac{\mu_1 Z_1}{Z} + \mu\right) R$$

$$D_{A2}(Z) = \frac{\alpha}{2} \int_{Z}^{\infty} \frac{dR}{R} e^{-\mu R} \int_{0}^{\infty} e^{-\mu_1 \frac{Z_1}{Z} R} \, d \, Z_1 = \frac{\alpha}{2\mu_1} \mu Z \, E_2(\mu Z) \qquad (65)$$

$$\approx \frac{\alpha}{2\mu_1} \frac{e^{-\mu Z}}{\mu Z} \qquad (66)$$

Problem 4.

Show that $J_{A2}(Z) = \frac{\alpha}{2\mu_1} (\mu Z)^2 E_3 (\mu Z)$ (67)

$$\cong \frac{\alpha}{2\mu_1} \frac{e^{-\mu Z}}{\mu Z} \qquad (68)$$

Problem 5.

Show that $J_{B2}(Z) = \frac{\alpha}{2\mu_1} \left[e^{-\mu Z} - E_3 (\mu Z) \right] \doteq \frac{\alpha}{2\mu_1} e^{-\mu Z}$ (69)

and that $D_{B2}(Z) \doteq \frac{\alpha}{2\mu_1} e^{-\mu Z}$ (70)

Hint: Use a buildup factor equal to the number of relaxation lengths in both shield and source, i.e. $B = \mu_1 R_1 + \mu R$.

---

c) Unshielded Semi-infinite Volume-distributed Source. It is now of interest to query what is the response of the detectors when placed next to this self-absorbing source, with no shield intervening. Setting $Z = 0$ in (69) and (70) we see at once that in case the attenuation in the source is exponential with linear buildup (a bad approximation for this case, since the effective number of relaxation lengths is small), then the dose as well as the current are $\frac{\alpha}{2\mu_1}$.

We are warned by the unreasonable appearance of an infinite answer that such a simple expedient is not possible for (66) and (68). Indeed this would not be expected to be the case in any event, since these expressions are for large argument, μZ, so we can hardly hope to use them for $\mu Z = 0$. We investigate the nature of $E_n(x)$ for small x.

$$E_n(x) = \int_x^\infty \frac{e^{-p}}{p^n}\, dp$$

For x small, the primary contributions are near the origin, so the exponential can be replaced by unity, and

$$E_n(x) \approx \int_x^\infty \frac{dp}{p^n} \approx \frac{x^{1-n}}{n-1}, \quad n \neq 1. \tag{71}$$

Using (71), we find that

$$D_{A2}(0) = \frac{\alpha}{2\mu_1} \tag{72}$$

$$J_{A2}(0) = \frac{\alpha}{4\mu_1} \tag{73}$$

Note the factor of two between $D_{A2}(0)$, the dose outside the source, and $J_{A2}(0)$, the number leaving per unit of source surface. The applicable expression will differ with receptor and the actual geometry. Thus, suppose we

had a large black object pressed against the source, and asked the dose received at the middle of the irradiated surface. Obviously J would be adequate, for this represents all the radiation available. On the other hand, a small not very absorbing object next to a large source would be affected according to D.

Line Source

It is occasionally of interest to calculate the flux from a non-self-absorbing source distributed along a line. For illustration of this method a case leading to an integrable form is chosen, but it is to be pointed out that this is not always possible and often the integration must be carried out by hand.

Line Source, Milligoat, Exponential Attenuation with Linear Buildup Factor.

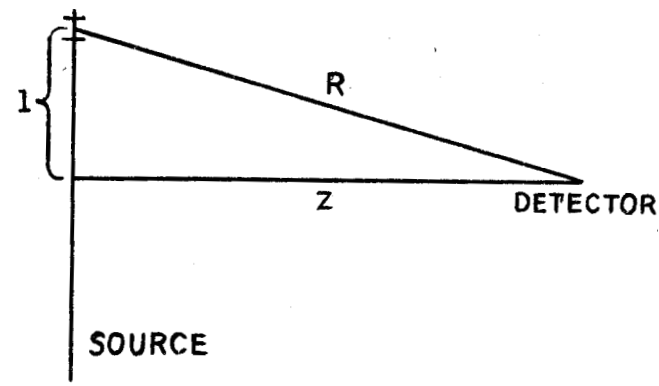

Figure 14

$$D(Z) = 2 \int_{\ell=0}^{\infty} d\ell \, \mu R \, \frac{e^{-\mu R}}{4\pi R^2}$$

Let $\mu R = x$; $\mu Z = c$; $d\ell = \dfrac{R \, d \, R}{\sqrt{R^2 - Z^2}}$

$$D(Z) = \frac{2\mu}{4\pi} \int_c^{\infty} \frac{x\, e^{-x}}{x^2} \frac{x\, dx}{\sqrt{x^2 - c^2}} .$$

Let $x - c = y$;

$$D(Z) = \frac{2\, e^{-c}}{4\pi\lambda} \int_0^{\infty} \frac{e^{-y}\, dy}{\sqrt{y(y + 2c)}} = \frac{\mu\, e^{-c}}{2\pi} e^{c} K_o(c)$$

For large argument, $K_o(c) \cong \left(\frac{\pi}{2c}\right)^{1/2} e^{-c}$

$$D(Z) \cong \frac{\mu}{2\pi} \sqrt{\frac{\pi}{2\,\mu\, Z}}\; e^{-\mu Z} \tag{74}$$

Note that this agrees, at least qualitatively, with the form of expression (37), in that the intensity varies with the square root of the distance in addition to the exponential attenuation.

- - -

EPB:lg
1/30/52

Revised
EPB:ms
9/29/52

REFERENCES

(1) T. W. Bonner, R. A. Ferrell, M. C. Rinehart, LA-715, February 8, 1949.

(2) D. W. Hill, CP-3800, April 14, 1947.

(3) B. E. Watt, LA-718, December 17, 1948.

(4) N. Feather, BM-148.

(5) N. Nereson, et al. LA-1078, March 8, 1950.

(6) D. J. Hughes, CF-3596, February 1, 1946.

(7) J. S. Levinger, E. P. Meiners, M. B. Sampson, A. H. Snell, and R. G. Wilkinson, CP-1967 (A-2844), July 29, 1944.

(8) M. Deutsch and Rotblat, LA-170, November 13, 1944.

(9) B. B. Kinsey, R. C. Hanna, and O. Van Patter, Canadian Journal of Research, 26A, 79(1948).

(10) K. Way and E. P. Wigner, Phys. Rev. 73, 1318 (1948).

(11) W. K. Ergen, ANP-59, May 3, 1951.

(12) L. E. Beghain, M. A. Grace, G. Preston, and H. Halban, Phys. Rev. 77, 286 (1950).

(13) M. A. Grace, L. E. Beghain, G. Preston, and H. Halban, Phys. Rev. 82, 969 (1951).

(14) E. T. Jarney, LA-1339, December, 1951.

(15) P. H. Stelson and W. M. Preston, Phys. Rev. 86, 132, (April 1, 1951), (February 13, 1951).

(16) E. P. Blizard and T. A. Welton, "The Shielding of Mobile Reactors," Reactor Science and Technology, Vol. 1, No. 3 (1951).

(17) R. Latter and H. Kahn, R-170, September 19, 1949.

(18) W. S. Snyder and J. L. Powell, ORNL-421, March 14, 1952.

(19) G. R. White, NBS-1003, May 13, 1952.

(20) C. M. Davisson and R. D. Evans, Rev. Mod. Phys. 24, 79 (1952).

(21) L. H. Gray, Proc. Roy. Soc. A1 22, 674 (1929) and L. H. Gray, Proc. Camb. Phil. Soc. 40, 72 (1944).

(22) C. W. J. Wende, "The Computation of Radiation Hazards," TNX-7, or N-609, or M-1324, January 17, 1944. This report was for years the bible of all shield designers. It is especially useful and complete in geometry.

(23) E. P. Blizard, Oak Ridge National Laboratory, CF 50-8-49, "Shielding of Nuclear Reactors, Lecture III, Geometry Transformations for Shielding," August 14, 1950.

(24) J. M. Stein, J. M. Burnam, H. L. F. Enlund, and P. R. Kasten, Homogeneous Reactor Experiment Quarterly Progress Report for Period Ending November 30, 1950. Section on "Geometrical Factors," page 62, ORNL-925.